National Oceanography Centre
NATURAL ENVIRONMENT RESEARCH COUNCIL

National Oceanography Centre

Internal Document No. 11

Investigation of the Liverpool Bay mixing front using POLCOMS

D L Norman, J M Brown,
L O Amoudry & A J Souza

2014

National Oceanography Centre, Liverpool
6 Brownlow Street
Liverpool
L3 5DA
UK

Author contact details
Email: danon@noc.ac.uk
Jebro@noc.ac.uk

DOCUMENT DATA SHEET

AUTHOR
NORMAN, D L, BROWN, J M, AMOUDRY, L O & SOUZA, A J

PUBLICATION DATE 2014

TITLE
Investigation of the Liverpool Bay mixing front using POLCOMS.

REFERENCE
Southampton, UK: National Oceanography Centre, Southampton, 38pp.
(National Oceanography Centre Internal Document, No. 11)
(Unpublished manuscript)

ABSTRACT

Liverpool Bay, northwest UK, is a region of freshwater influence and hypertidal conditions. The river inflow from the 3 large estuary systems (Dee, Mersey and Ribble) forms a coastal front that moves < 10 km in response to semi-diurnal tidal straining and < 35 km due to the spring-neap cycle. The time variability of the density gradients in this coastal region are mainly controlled by salinity. Coastal observations are used in this study to improve the numerical simulation of the exchange process occurring at this front through improved spatial structure and temporal variability. A decade of Conductivity Temperature Depth (CTD) sensor observations were collected during cruises across a nearshore grid of monitoring stations. These data are used in addition to fixed mooring data that are near-continuous in time to validate numerical simulations using the 1-way nested Proudman Oceanographic Laboratory Coastal Ocean Modelling System (POLCOMS) at ~1.8km and 180m horizontal resolution. A downscaled simulation is used to investigate the influence of model resolution, inclusion of wetting and drying, diffusivity, turbulence advection and the influence of model boundary and initial conditions for select cruise periods in 2008. This year is chosen as a typical year with periods of calm and stormy conditions with variable river influence to investigate the seasonal frontal structure. A method to validate the spatial structure of the front is presented demonstrating the importance of a fine-resolution grid and improved physics to capture the details.

KEYWORDS

ISSUING ORGANISATION
National Oceanography Centre
University of Southampton Waterfront Campus
European Way
Southampton SO14 3ZH
UK

Page intentionally left blank

1. Introduction

Liverpool Bay in the NW of the UK is a shallow, hypertidal region of freshwater influence (ROFI), that is, in addition to the fast tidal currents, the dynamics of the region are strongly influenced by estuarine outflow (Simpson et al, 1990). Hypertidal is defined as a spring tidal range in excess of 6m (Dyer, 1997). Stratification is found to be dominated by salinity, though river temperature does have a seasonal effect (Polton et al, 2011). Souza (2013) clearly shows the occurring fronts in the region are: the Irish Sea front west of the Isle of Man, the Celtic Sea front and the Liverpool Bay front. A local modelling study of Liverpool Bay over the year 2008 is conducted to investigate the processes influencing the location of this tidally-mixed front, which is created by the freshwater inflow from three large estuary systems (the Dee, Mersey and Ribble).

I will be applying the nested Proudman Oceanographic Laboratory Coastal Ocean Modelling System (POLCOMS), with a 180m horizontal resolution and 20 sigma levels in the vertical, to Liverpool Bay (Fig.1) and comparing annual model simulations. (For full details of POLCOMS, refer to Holt and James, 2001.) A sensitivity analysis of the model to river salinity and temperature will be performed in order to identify the best setup. This setup will then be used in an investigation into the effects of including turbulence advection and horizontal diffusion in the model on the positioning of the local tidal mixing front within Liverpool Bay. We also test the model sensitivity to other parameter settings, such as river temperature, river salinity, mixing length scales and boundary conditions.

Figure 1: Locations of Sites A and B in Liverpool Bay (http://cobs.noc.ac.uk/cobs/fixed/).

The model is set-up on a B-grid and runs in a baroclinic mode (Holt and James, 2001). The sea surface is forced by hourly wind and pressure data and three-hourly cloud, precipitation, humidity and air temperature data from the UK MESOSCALE Met Office model. The archived National Oceanography Centre's Coastal Observatory (CObs) pre-operational model provides the boundary forcing for velocity, elevation, temperature and salinity, in addition to the initial density field (generated from initial temperature and salinity conditions). This pre-operational model provides initial conditions that have been spun up over multiple years, thus avoiding great computational cost if spun up from constant values for this study. CObs was a 10-year observational programme that provides data with which POLCOMS can be validated against (Howarth and Palmer, 2011). It has been shown that POLCOMS performs well in predicting surface temperature and salinity, though more accurately temperature (O'Neill et al, 2012). River flow is forced by daily averaged discharge data available from the UK National River Flow Archive. POLCOMS is coupled to the Global Ocean Turbulence Model (GOTM) to represent vertical mixing using the k-epsilon scheme (Canuto et al., 2001).

The study focuses on the year 2008, using December 2007 as the spin-up month. Analysis of distribution histograms over this annual period shows that 2008 is a typical year in atmospheric, riverine and coastal conditions so is suitable for this study (Norman et al., 2014b).

POLCOMS applied to the Irish Sea (IRS), with a 1.8km horizontal resolution and 32 sigma levels in the vertical, provides the boundary forcing for the higher resolution Liverpool Bay (LB) model. The LB model has less vertical levels to avoid errors as a result of the inclusion of wetting and drying, whereas the IRS model has a minimum depth of 5m. Applying more sigma levels in the very shallow regions of the LB model would be unrealistic as the vertical resolution would be less than the bed roughness length causing unphysical errors in wetting and drying cells. A previous study (Norman et al., 2014a) identified the best model setup for the IRS to be: river outflow salinity set to 20psu, and river temperature included. It was also shown that in order to decrease run time, the same setup can be run without waves included with little impact on model performance.

Both IRS and LB model simulations are validated against data recorded in Liverpool Bay by CObs.

2. Modelling Methods

To assess model performance, each simulation is validated against data recorded at Sites A and B (Fig. 1) using matlab scripts validation_siteA_LB.m and validation_siteB_LB.m[1] respectively. These scripts read in both the simulated model data and observed data into arrays, compute error metrics: bias of the mean, root mean squared error (RMSE) and model skill following Willmott (1981), and extract and plot annual time series for temperature, salinity, density and density difference.

Sites A and B are detailed in Howarth and Palmer (2011), but briefly they were established as part of CObs, with Site A being located close to where the outflow from the river Mersey enters Liverpool Bay and Site B being installed to enable calculation of horizontal gradients between the two locations.

The bias of the mean, RMSE and model skill are calculated using get_bias_array.m, get_rmse_array.m and Model_Skill_array.m[2] respectively.

The bias is defined as:

$$Bias = \bar{M} - \bar{O}$$

where M represents the model values, O the observed values and $\overline{X} = \frac{1}{n}\sum_{k=1}^{n} X_k$. A value of 0 corresponds to an unbiased estimator; a positive value implies positive bias, that is, the model is over-predicting and a negative value implies negative bias or under-predicting.

The RMSE is defined as:

$$RMSE = \sqrt{\overline{(M-O)^2}}$$

where a smaller value indicates better model performance, and the model skill is defined as:

$$D = 1 - \frac{\overline{(M-O)^2}}{\overline{(|M-\bar{O}| + |O-\bar{O}|)^2}}$$

D takes values between 0 and 1, where 0 implies no agreement and 1 implies total agreement.

These error metrics were also used in the validation of the IRS model (Norman et al., 2014a).

[1] These scripts can be found at: /projectsa/iCoast/Mersey_CEFAS/LB2008/matlab
[2] These scripts can be found at: /projectsa/iCoast/Mersey_CEFAS/LB2008/matlab/functions

2.1 Boundary Forcing

In a previous POLCOMS modelling study of the Irish Sea in 2008 (Norman et al., 2014a), it was shown that salinity and therefore density is under-predicted due to river inflow salinity being provided by a climatological river, rather than true data. The initial bias in salinity was calculated between the first data point and the corresponding model value at 5 and 10m below the surface and 0.5m above the bed at both Sites A and B. The average of these differences was found to be -1.15psu so in order to provide the best boundary forcing for the nested LB model, the IRS model control setup (20psu river salinity; river temperature included) was run with its initial salinity conditions biased by +1.15psu. This led to an increase in salinity (and density) over the full annual period, not only the initial months (Figs. 2 and 3) improving the model simulation.

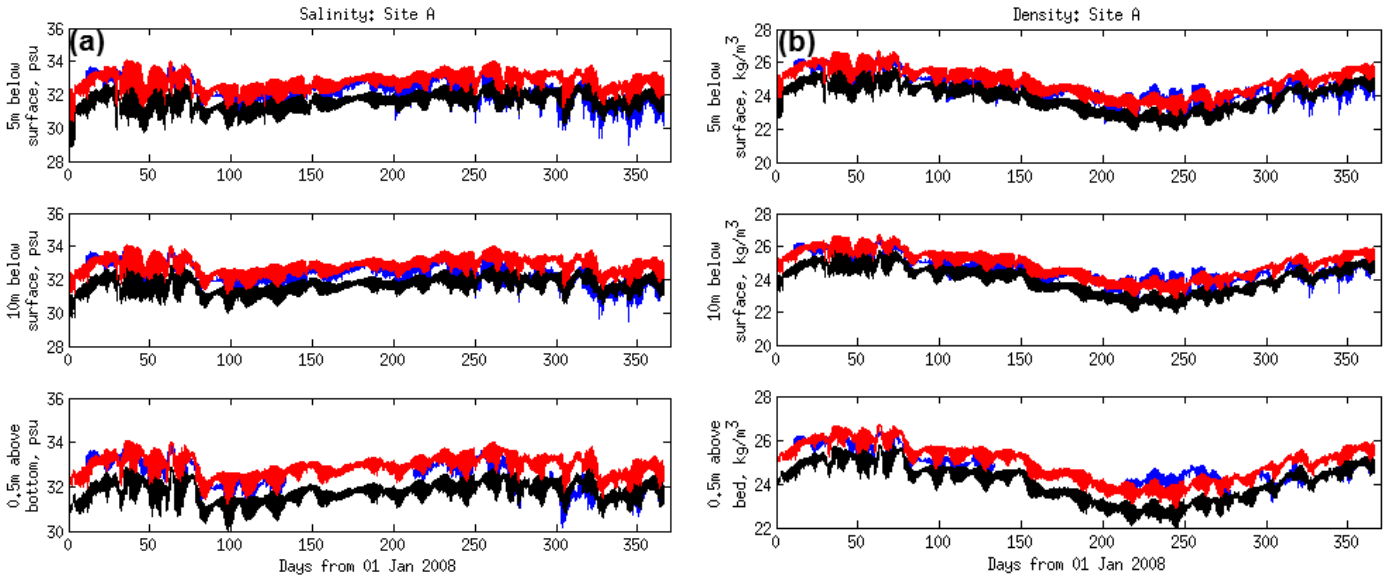

Figure 2: Annual (a) salinity and (b) density model outputs with (red) and without (black) an initial salinity bias of 1.15psu and observed (blue) data, at Site A.

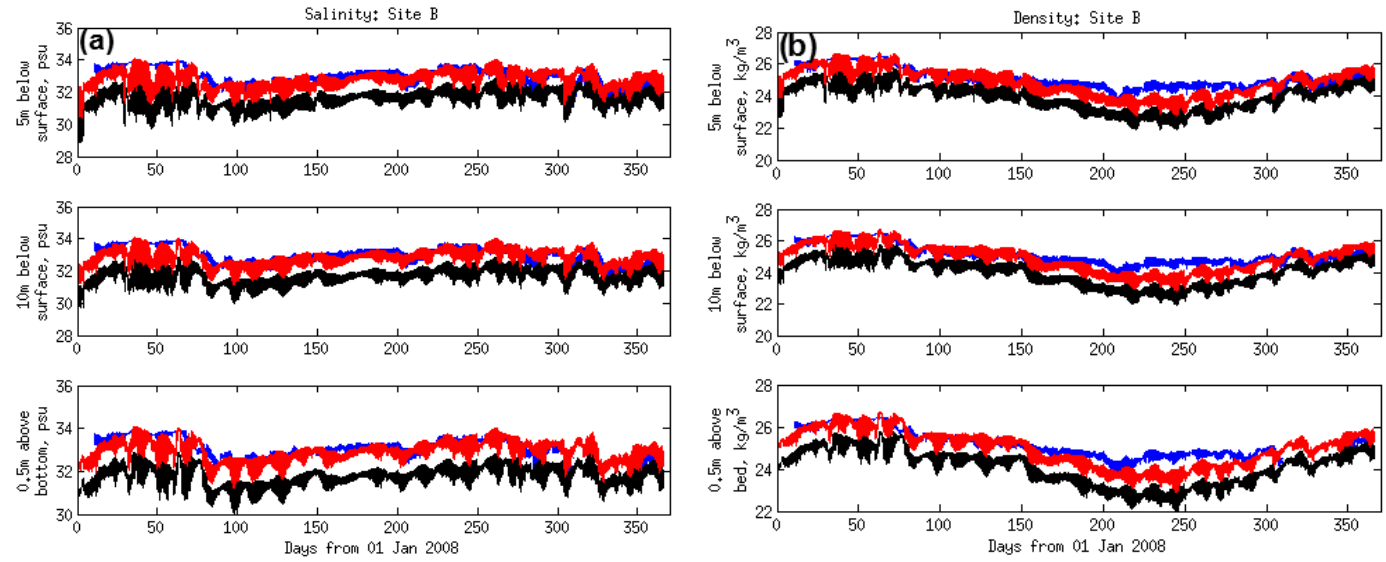

Figure 3: Annual (a) salinity and (b) density model outputs with (red) and without (black) an initial salinity bias of 1.15psu and observed (blue) data, at Site B.

Table 1 shows the error metrics calculated for the biased IRS model run. The model is now positively biased, but to a lesser extent than it was previously negatively biased. Generally, the model skill has improved and is greater than 0.6 in all instances suggesting good predictive capability, and the RMSE has decreased.

Table 1: Error metrics for Site A and Site B: IRS biased run. U and v denote the velocity components, S salinity, T temperature and ρ density.

IRS: bias 1.15psu		Site A			Site B		
		Model Skill	Bias	RMSE	Model Skill	Bias	RMSE
	u	0.96	0.02	0.15	0.98	0.02	0.11
	v	0.81	0.01	0.07	0.87	0.00	0.06
	-5m	0.66	0.57	0.57	0.62	0.65	0.42
S	-10m	0.69	0.51	0.48	0.62	0.62	0.37
	Bottom	0.72	0.39	0.54	0.63	0.55	0.31
	-5m	0.96	0.21	1.71	0.96	0.48	1.50
T	-10m	0.96	0.28	1.66	0.96	0.47	1.47
	Bottom	0.95	1.05	1.86	0.96	0.34	1.48
	-5m	0.90	0.35	0.41	0.88	0.37	0.38
ρ	-10m	0.92	0.29	0.38	0.88	0.36	0.36
	Bottom	0.90	0.05	0.50	0.91	0.33	0.33

Table 2 shows the same error metrics calculated for the LB control setup. We can see that this higher resolution model shows increased skill in replicating sea temperature at the two mooring sites, but reduced skill in salinity and density, which are now being further over-predicted. This could be due to the higher resolution requiring more processes and inputs in order for it to perform better. This is later investigated in Section 4.4.

Table 2: Error metrics as per Table 1, for Site A and Site B: LB control run.

LB: control		Site A			Site B		
		Model Skill	Bias	RMSE	Model Skill	Bias	RMSE
	u	0.97	0.00	0.14	0.98	0.01	0.11
	v	0.82	0.01	0.07	0.92	0.00	0.05
	-5m	0.45	1.08	0.74	0.42	0.98	0.56
S	-10m	0.42	1.03	0.70	0.41	0.95	0.53
	Bottom	0.46	0.92	0.76	0.38	0.87	0.50
	-5m	0.99	0.43	0.75	0.98	0.54	0.67
T	-10m	0.99	0.48	0.75	0.98	0.54	0.68
	Bottom	0.99	1.24	1.07	0.98	0.41	0.73
	-5m	0.69	0.74	0.53	0.71	0.65	0.42
P	-10m	0.69	0.70	0.50	0.71	0.62	0.40
	Bottom	0.71	0.46	0.56	0.76	0.58	0.37

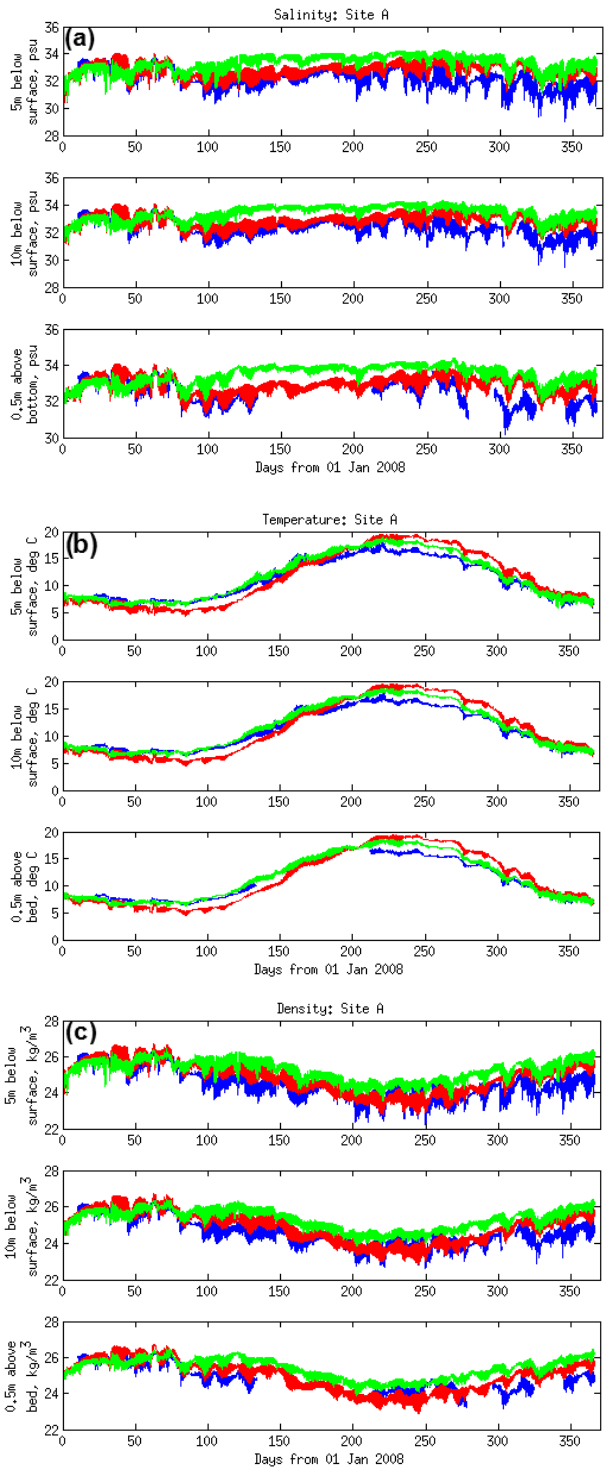

Figure 4: Annual (a) salinity, (b) temperature and (c) density model outputs for the biased Irish Sea (red) and Liverpool Bay control (green) runs with observed (blue) data, at Site A.

In Figure 4, the IRS model is visibly more accurate at replicating the observed salinity and density data at Site A, whereas the LB model performs better for temperature.

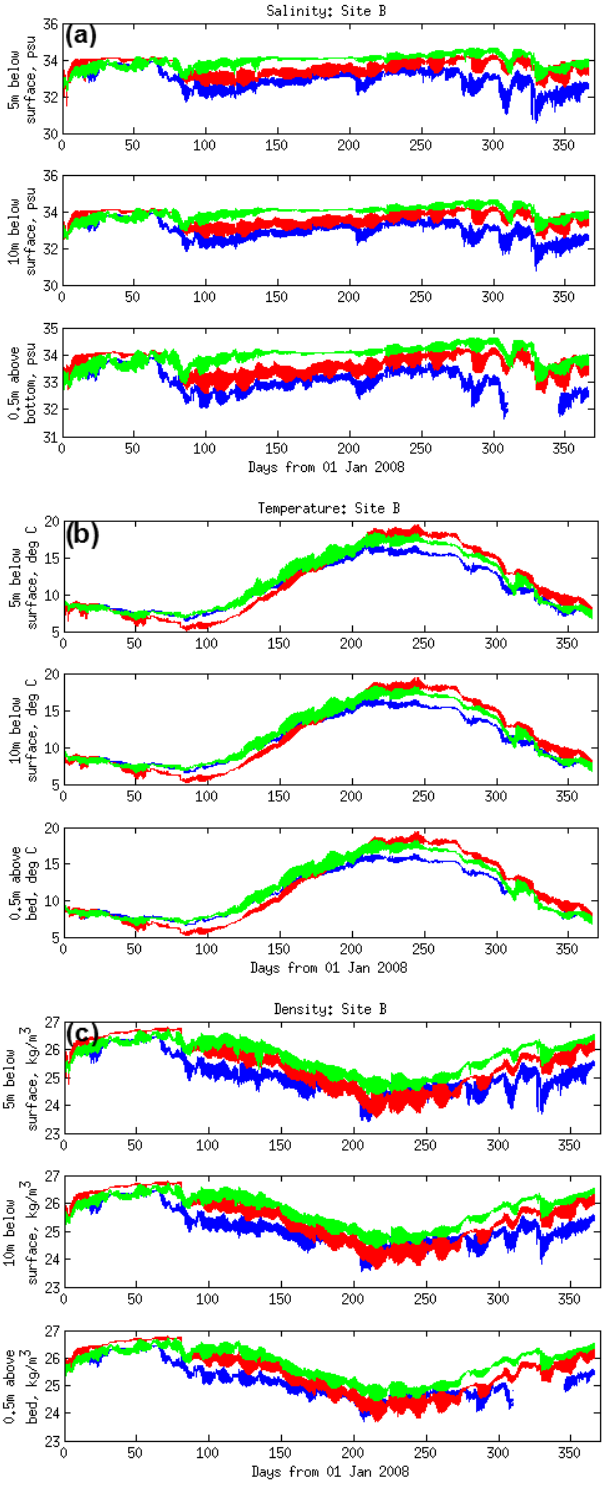

Figure 5: As for Figure 2, at Site B.

Figure 5 again shows that the IRS model is performing better in salinity and density predictions, but not so in temperature. Also at Site B, a significant drop in salinity of approximately 2psu between days 66 and 87 in March was observed (Fig. 5a), but this is not sufficiently captured by either model, especially LB. This is examined further in Section 4.

3. Sensitivity Analysis

For the sensitivity analysis of the LB model, four executables[3] were compiled (Table 3). The configuration elements in bold highlight the test parameter for each model run. In the LB control setup, river salinity is set to 0psu (not 20psu as for IRS) as the higher resolution means the estuaries are resolved.

Table 3: Model configuration and name for each simulation. The two investigations are colour coded as follows, red: the effect of river temperature; and green: the effect of river source salinity.

Run name	Executable name	Configuration
control	mobius_hydro	▪ **river temperature on** ▪ **0psu river salinity**
norivtmp	mobius_norivTMP	▪ **river temperature off** ▪ 0psu river salinity
5psu	mobius_5psu	▪ river temperature on ▪ **5psu salinity**
10psu	mobius_10psu	▪ river temperature on ▪ **10psu salinity**

River salinity was altered in "Freshwater.F" and river temperature was switched off using the "NORIVTMP" compile option. The river temperatures used in the control run are in fact atmospheric temperature used as proxies for river temperature, taken from a land point close to the river source (Norman et al., 2014a).

3.1 River Temperature

Figure 6 shows sea temperature at sites A and B for both the control (river temperature included) and norivtmp (river temperature switched off) model runs, together with observational data. The exclusion of river temperature has little effect, with its main impact being on the bottom water. This was also evident in the IRS sensitivity analysis (Norman et al., 2014a) where it was shown that the rivers are having a warming influence on sea temperature during winter months and a cooling effect from late spring and into summer. The river inflow in January, for example, in norivtmp is therefore cooler than that in the control. This slightly denser water acts to weaken stratification and enhance mixing. This may explain why the effect is greater in the bottom water, as the river water is mixed throughout. Conversely, in the summer (days 183-274), when control is cooler, the opposite occurs – warmer river temperatures act to increase the buoyancy (reduce density) and enhance stratification.

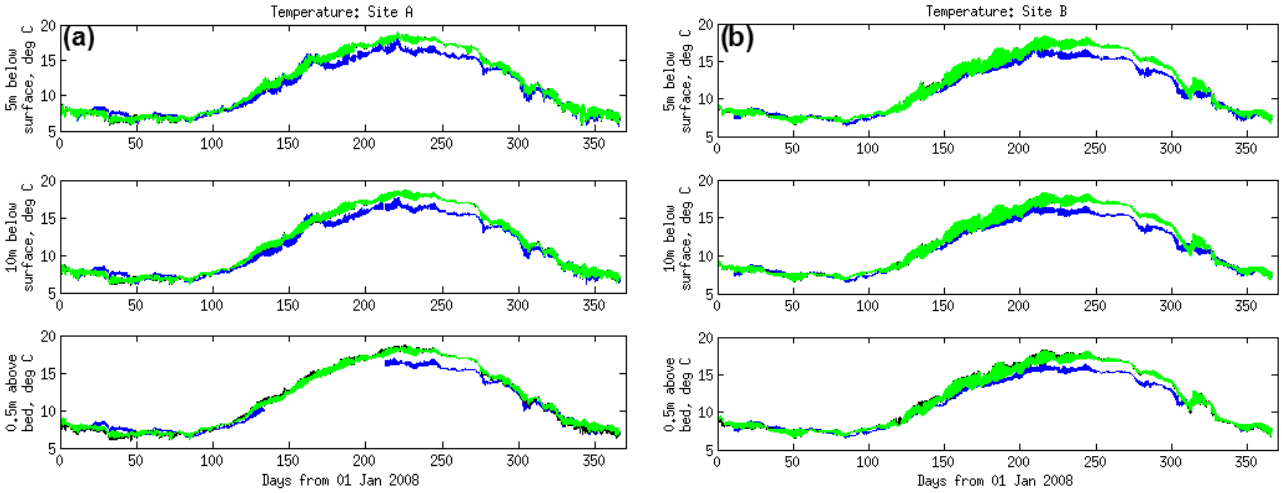

Figure 6: Annual temperature time series for control (green), norivtmp (black) and observations (blue) at (a) Site A and (b) Site B.

[3] Executables can be found at: /projectsa/iCoast/Mersey_CEFAS/LB2008/Danielle

Table 4 contains the error metrics for temperature at sites A and B for both the control and norivtmp simulations. The model skill is unaffected by the exclusion of river temperature though the bias is reduced slightly at Site A and the RMSE is reduced at site B. As the estuarine circulation is not modified significantly by temperature, the salinity validation (not shown) is unchanged offshore. The density shows negligible change in performance, as expected, since it is dominated by salinity. As including the river temperature proxies has no significant impact on the error metrics or model performance, it is included to make the model more realistic by representing the seasonal cycle.

Table 4: Error metrics for sea temperature at Sites A and B: control and norivtmp. The values representing best model performance are highlighted in bold.

TMP	Run	Model Skill			Bias			RMSE		
		-5m	-10m	0.5m	-5m	-10m	0.5m	-5m	-10m	0.5m
Site A	control	0.99	0.99	0.99	0.43	0.48	1.24	**0.75**	0.75	1.07
	norivtmp	0.99	0.99	0.99	**0.41**	**0.46**	**1.23**	0.76	0.75	1.07
Site B	control	0.98	0.98	0.98	0.54	0.54	0.41	0.67	0.68	0.73
	norivtmp	0.98	0.98	0.98	0.54	0.54	0.41	0.67	**0.67**	**0.72**

3.2 River Salinity

To measure the effect of river salinity on the model, the salinity at sites A and B from the control run (0psu) is compared with that from setups with the river salinity set to 5psu and 10psu.

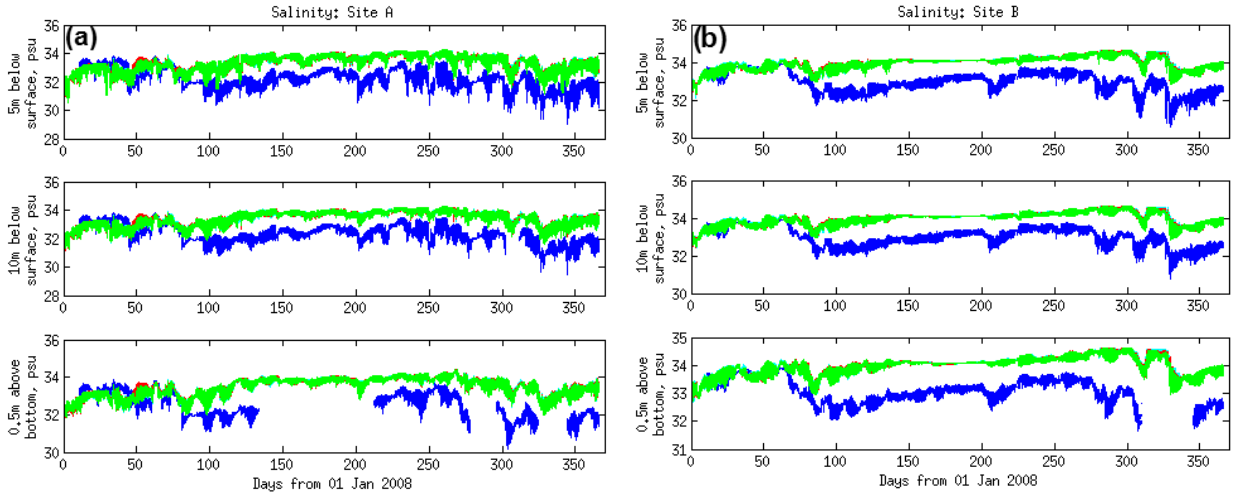

Figure 7: Annual salinity model outputs for the control (green), 5psu (red) and 10psu (cyan) setups, and observations (blue) at (a) Site A and (b) Site B.

Figure 7 shows that increasing the river salinity by 5 or 10psu has little effect on the modelled salinity at Sites A and B, only fractionally adjusting it at certain times throughout the year. Table 5 supports this, with variations in the error metrics from the control run being a maximum of 0.3 in the bias at 5m below surface level for both sites. Changes in the salinity are likely to change the estuarine density gradients, but offshore the impact is minimal as the extent to which the freshwater plume travels into Liverpool Bay is unchanged. Table 5 shows that the control setup remains most valid.

Table 5: Error metrics for salinity at Site A and Site B: LB control, 5psu and 10psu setups. The values representing best model performance are highlighted in bold.

SAL	Run	Model Skill			Bias			RMSE		
		-5m	-10m	0.5m	-5m	-10m	0.5m	-5m	-10m	0.5m
Site A	control	**0.45**	**0.42**	**0.46**	**1.08**	**1.03**	**0.92**	0.74	0.70	0.76
	5psu	**0.45**	**0.42**	**0.46**	1.11	1.05	0.94	**0.73**	**0.68**	**0.75**
	10psu	0.44	0.41	0.45	1.11	1.06	0.94	0.74	0.69	0.77
Site B	control	**0.42**	**0.41**	**0.38**	**0.98**	**0.95**	**0.87**	**0.56**	**0.53**	**0.50**
	5psu	0.41	**0.41**	0.37	1.00	0.97	0.88	0.57	0.54	0.51
	10psu	0.41	**0.41**	**0.38**	1.01	0.98	0.89	0.57	0.54	**0.50**

4. Mixing Front Investigation

4.1 Introduction

During the CObs campaign, a survey grid of 34 CTD sites (providing conductivity, temperature and pressure measurements) was established (Fig. 8) and visited on an approximately monthly basis in 2008. Owing to the availability of this data and periods identified in Norman et al. (2014b) as suitable periods to study, the cruises that took place in January (10^{th}-11^{th}), May (13^{th}-16^{th}) and July (30^{th}-31^{st}) will provide the basis of the investigation into the positioning of the mixing front within Liverpool Bay.

January experienced the highest river flows seen during 2008 accompanied by stormy conditions. A study in this month allows us to see how the front is affected by these influences. Towards the end of May, the conditions were calm with low river outflow, in contrast to the January conditions.

Ideally, September would have been used as the final month of investigation as an example of calm conditions with high river outflow, for comparison with the previous months. Unfortunately, there is no cruise data for this month so the July cruise, which visited all of the sites, was chosen. Towards the end of July, the weather was calm with moderate river flow (Norman et al. 2014b).

As each survey takes 2 to 3 days to complete, the data collected is representative of the full tidal cycle and not a particular snapshot in time. Unfortunately, variability during different phases within the cycle is not captured and can only be investigated using model simulation (Section 4.7).

A list of the CTD site locations can be found in Appendix 1 and the sites visited on each of the three cruises studied here in Appendix 2.

The full 2008 cruise data can be found at: /projectsa/iCoast/Mersey_CEFAS/observation/CTD/2008_all.

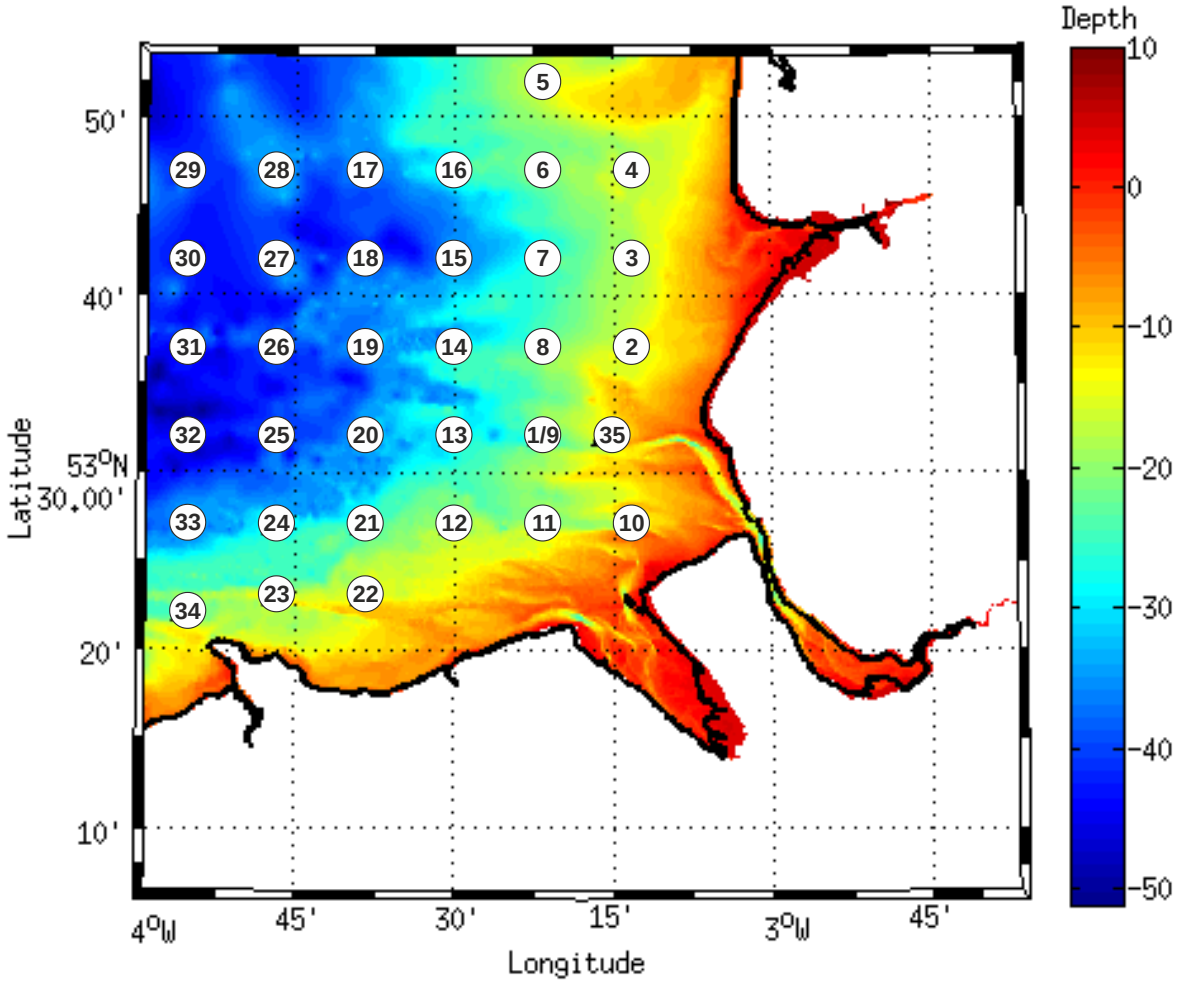

Figure 8: Depth (m) in Liverpool Bay with the CTD site locations marked and numbered.

Table 6: The CTD sites comprising the full transects defined as 1 to 5.

Transect	Sites					
1	29	28	17	16	6	4
2	30	27	18	15	7	3
3	31	26	19	14	8	2
4	32	25	20	13	1/9	35
5	33	24	21	12	11	10

4.2 Methods

read_CTDdata.m reads in cruise data files and extracts time, longitude, latitude, pressure, salinity, temperature and potential density, storing them in arrays according to site number. Pressure is used as a proxy for depth here as they are equivalent at these depths. The temperature, salinity and density observations are then interpolated onto sigma levels to be comparable with the model data. The data is plotted as 5 transects (Table 6), except for January when only 3 of the 5 were observed. It should be noted that the sites along a given transect were not always visited consecutively.

read_modelCTD.m reads in temperature and salinity data outputted by each model run, then uses the times from the cruise data to extract the corresponding model data from the same location at the nearest model time point that each site was visited on the cruises. Density is calculated using the UNESCO equation of state and the data is again plotted as transects.

Both observational and model transect data is read in using CTD_validation.m and error metrics calculated to validate the model. The squared buoyancy or Brunt–Väisälä frequency, a measure of the stability of stratification, is calculated both across the transect (x-direction in CTD figures) at each sigma level and vertically through the water column (y-direction in CTD figures) at each site location. In attempt to capture the model's capability at representing the structure of the front, this was calculated for each increment of a transect, prescribed by the CTD grid resolution in the horizontal, and between each sigma level as prescribed by the model resolution in the vertical. The model skill, cost function and Pbias are then calculated using these values for both the model and observational data sets. These metrics indicate the model capability at simulating the gradients in a chosen variable (e.g. density in this case) across the ROFI.

The squared buoyancy frequency (N^2) is defined as:

$$N^2(x) = \frac{d\rho}{dx} \times \frac{-g}{\rho_0},$$

where x is the horizontal or vertical grid increment, g is the acceleration of gravity (9.81m/s^2) and ρ_0 is the potential density (999.842594kg/m^3). In order for the horizontal density gradient between each site to be calculated, the longitude and latitudes of each site were converted into Eastings and Northings and the distance between them found in metres. For the vertical gradient, the depth between each sigma level was calculated by dividing the elevation at the required instance for each site by the number of sigma levels, i.e. 20. In the vertical a value less than zero indicates that the stratification is stable and where greater than zero, unstable. When applied in the horizontal direction, a positive N^2 indicates decreasing density from west to east towards the coastal freshwater sources, and zero indicates horizontally well mixed. A negative value should not occur for this study application.

As the N^2 values in both directions were to the order of 10^{-5} or 10^{-7}, the resulting bias and RMSE were also very small and therefore not useful in conveying the model's performance. The following error metrics were chosen for providing sensible numbers for analysis.

The cost function (Allen et el., 2007) is defined as:

$$CF = \frac{1}{n}\sum_1^n \frac{|O_n - M_n|}{\sigma_O},$$

where O represents the observed values, M the model, and σ is standard deviation. The cost function is a measure of ratio of the model data misfit to a measure of the variance of the data; the closer the value is to zero the better the model. The CF values are measured against the following classifications:

<1	Very good
1-2	Good
2-3	Reasonable
>3	Poor

The percentage model bias, which indicates the tendency of the model values to be greater or less than the observed, is defined (Allen et el., 2007) as:

$$Pbias = \frac{\sum_1^n (M_n - O_n)}{\sum_1^n |O_n|} * 100,$$

where a value of zero is optimal, indicating no bias. Allen (2007) does in fact use the sum of the observed-model values, but to be consistent with my previous bias calculations, I am using the reverse so that a positive Pbias equates to over-prediction by the model, and a negative Pbias to under-prediction. I have also used the absolute values in the denominator to ensure the sign of the Pbias is determined by the sign of the error.

4.3.1 The transects: observations

Figures 9-11 show the observed density seen in January, May and July, respectively, interpolated onto the model sigma levels[4]. These plots will be used for a visual comparison with the model outputs.

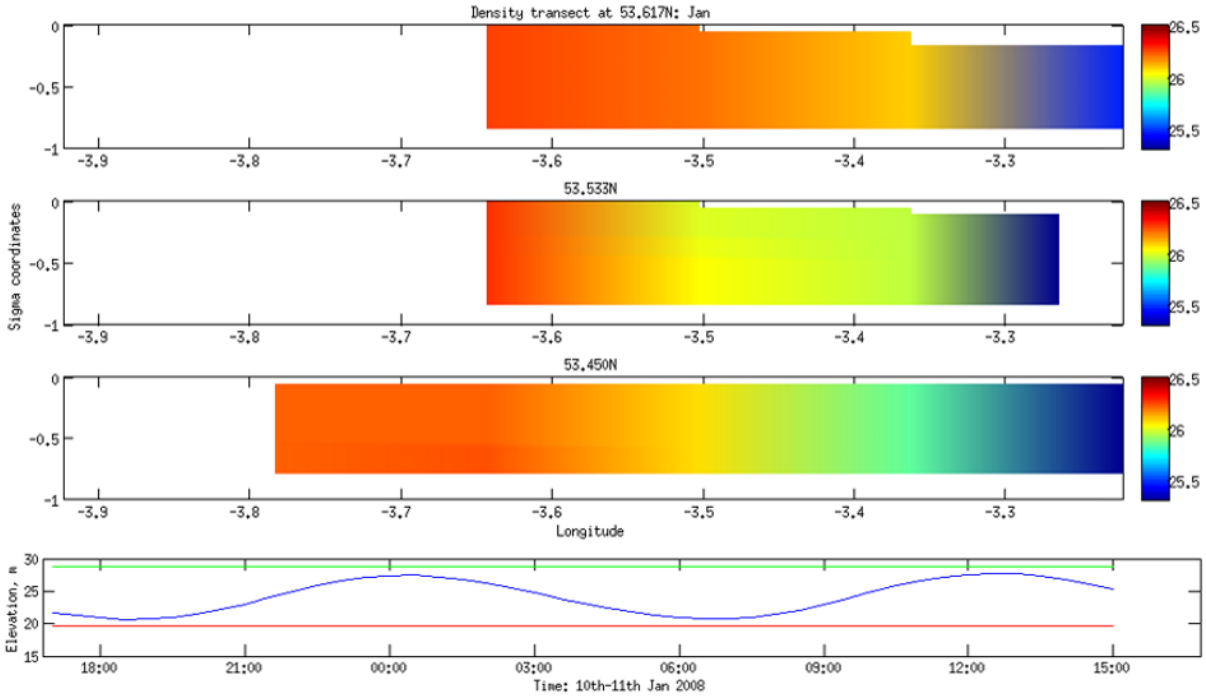

Figure 9: Transects 3 (top panel)-5 (bottom panel) displaying observed density in January interpolated onto the model sigma levels. The bottom plot displays model tidal elevation (blue) for the duration of the cruise along with the maximum (green) and minimum (red) elevations seen in 2008.

January (Fig. 9) shows the water column to be consistently vertically mixed, with density increasing in the horizontal with distance from the coast. The tidal dynamics during this cruise are representative of spring tide conditions. In the absence of a freshwater plume (seen in both summer months), the more saline seawater is not pushed offshore in the surface layers as a result of the river influence causing the near-shore to be more dense than seen in May or July.

[4] The transect plotting/validation scripts can be found at: /projectsa/iCoast/Mersey_CEFAS/LB2008/matlab

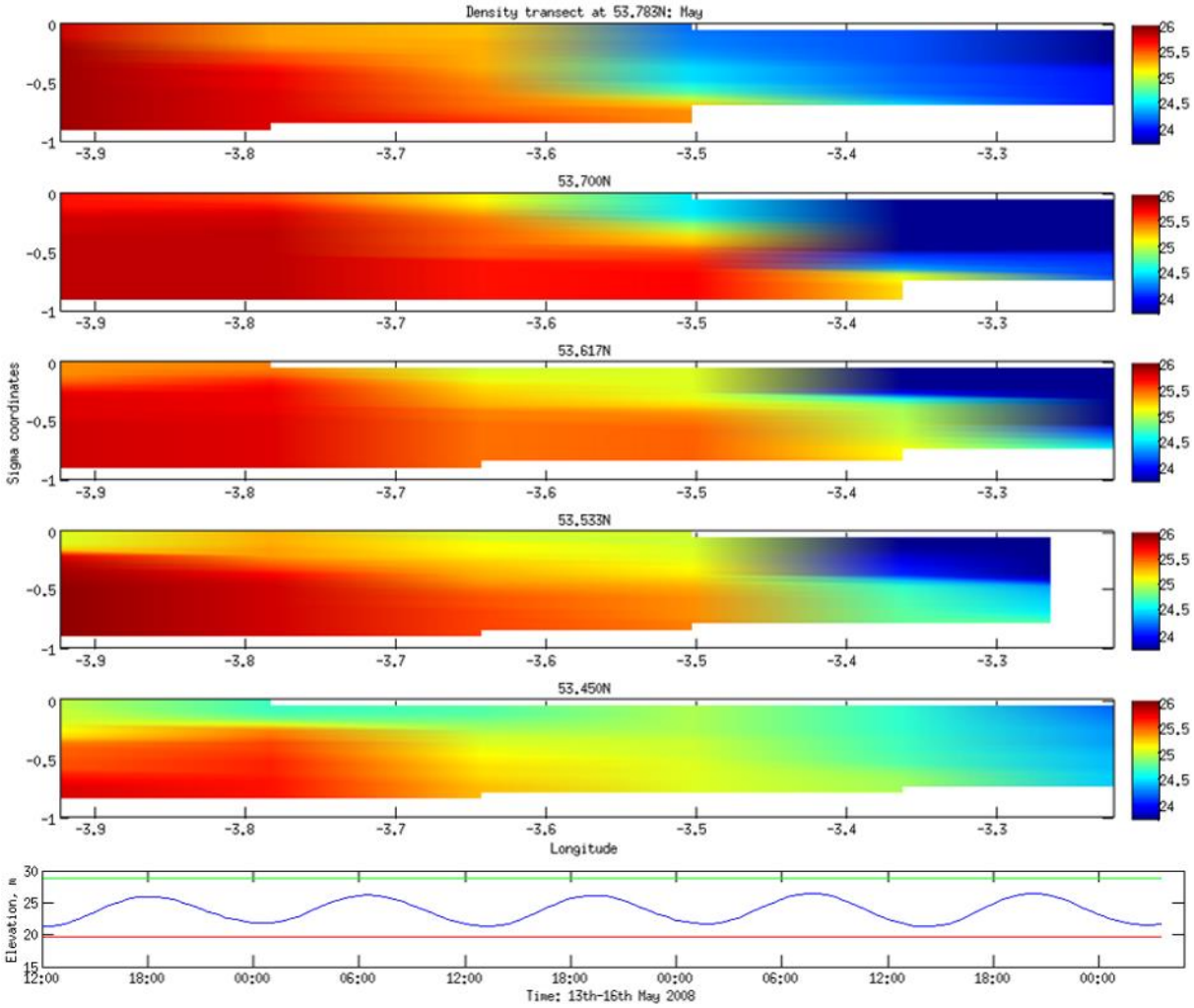

Figure 10: Transects 1 (top panel)-5 (bottom panel) displaying observed density in May interpolated onto the model sigma levels. The bottom plot displays model tidal elevation (blue) for the duration of the cruise along with the maximum (green) and minimum (red) elevations seen in 2008.

In May (Fig. 10), we see the influence of the warm, fresher river water creating stratification during neap tide conditions. The surface plume extends further west in the north of Liverpool Bay, owing to the outflow from the rivers Mersey and Ribble, with the influence of the river Dee evident in the stratification extending further west in the most southerly transect. In Liverpool Bay the Coriolis Effect causes the freshwater plumes to spread north merging along the coast (as seen later in Fig. 17). We can also see that water across the southernmost transect is less dense than in the north, and the stratification occurs further offshore here; the surface plume is less disperse. The seasonal solar heating of the sea surface creating temperature-driven stratification (not shown) also occurs during May.

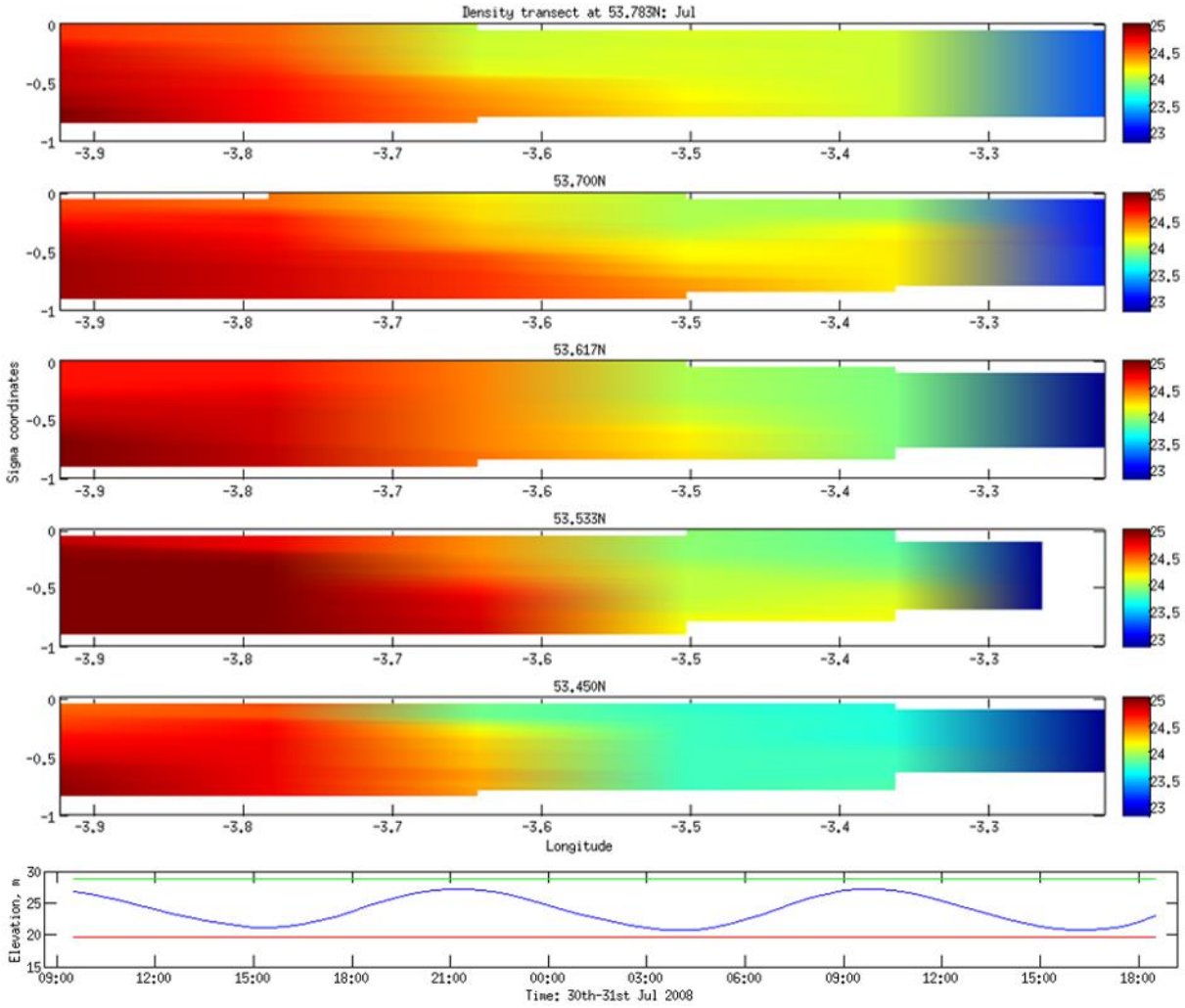

Figure 11: Transects 1-5 displaying observed density in July interpolated onto the model sigma levels.

Again, stratification is visible in July (Fig. 11), but the extent of the front into the bay is reduced; the water column is mixed at the most easterly longitudes with stratification occurring around -3.6 to -3.4°W in transects 1-4, and slightly further west in transect 5. The shape of the front is clearly shown in the July transects. The influence of the freshwater from the Dee and Mersey estuaries is evident in transect 5 with the front being pushed further east. During this cruse the tidal regime is considered to represent mean tidal condition.

The cruise in January occurred at spring tide (Fig. 9) so the water is possibly more mixed due to more energetic tidal mixing. Whereas in May (Fig. 10), the cruise occurred around neap tide and the water is more stratified. Figure 11 shows that the July cruise took place at mean tide, between spring and neap, and the transects also show profiles between those of January and May with a mixture of well-mixed and stratified water. Earlier studies (Hopkins and Polton, 2012) have identified three regimes (vertically mixed, bottom-attached and bottom-detached plume dynamics) in response to seasonal heat fluxes. Further analysis of model transects at different stages of the spring-neap cycle for a given month is required to confirm the plume development is, as suggested, related to the tidal dynamics and not seasonal heating.

4.3.2 The transects: model

The control setup as detailed in Section 3 was used to create corresponding transects of model data to the observations (Figs. 12-14).

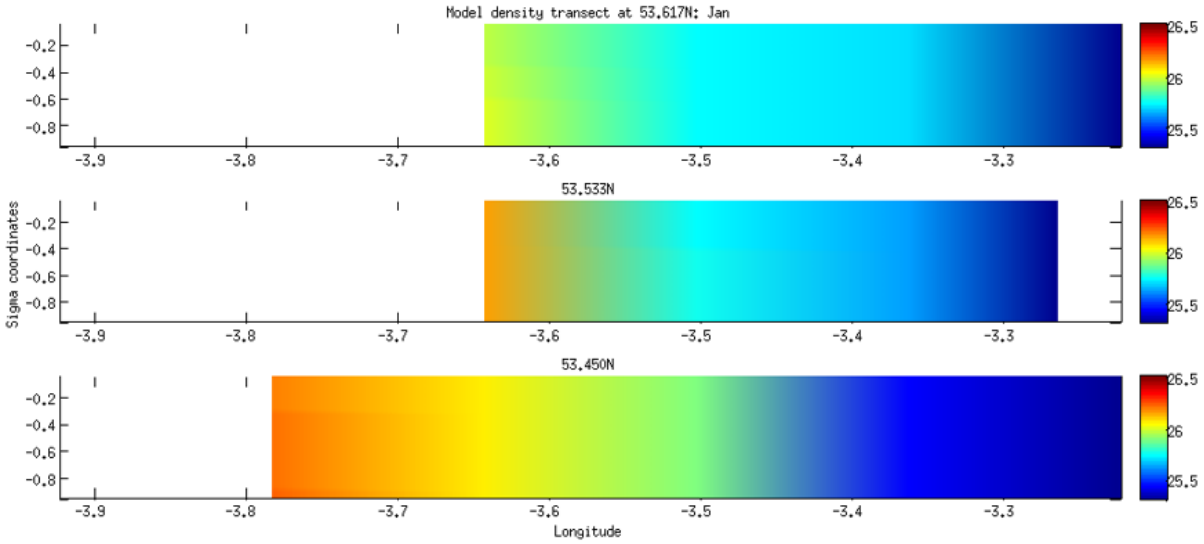

Figure 12: Transects 3-5 displaying model density on sigma levels in January.

Figure 12 shows that the model density in January does replicate the pattern of the observations (vertically well mixed), but everywhere bar the most easterly point in the transect is too fresh – the model correctly simulates a vertically well mixed water column, but the freshwater extends too far offshore. The high model skill in the horizontal reflects this capacity to capture the horizontal gradient (Table 7). Transect 5 is best replicated but the plume is just slightly further offshore in the model. The cost function is low in all instances except transect 3 in the vertical. This also coincides with a large Pbias value, which shows that this calculation is possibly unreliable in mixed water when there is only limited data available. As the water column is well mixed, the vertical N^2 values (the sum of which constitutes the denominator in the Pbias calculation) tend to 0, causing the Pbias values to tend towards +/-infinity.

The Pbias shows the horizontal density gradients are being over-predicted in January.

Table 7: Error metrics for density transects 3-5 of the LB control run in January.

	HORIZONTAL			VERTICAL		
CTD: Jan DENSITY	Model Skill	Pbias	CF	Model Skill	Pbias	CF
3	0.82	61.37	0.95	0.12	-351.62	2.79
4	0.82	64.20	0.96	0.64	39.74	0.31
5	0.91	46.06	0.58	0.22	95.54	0.35

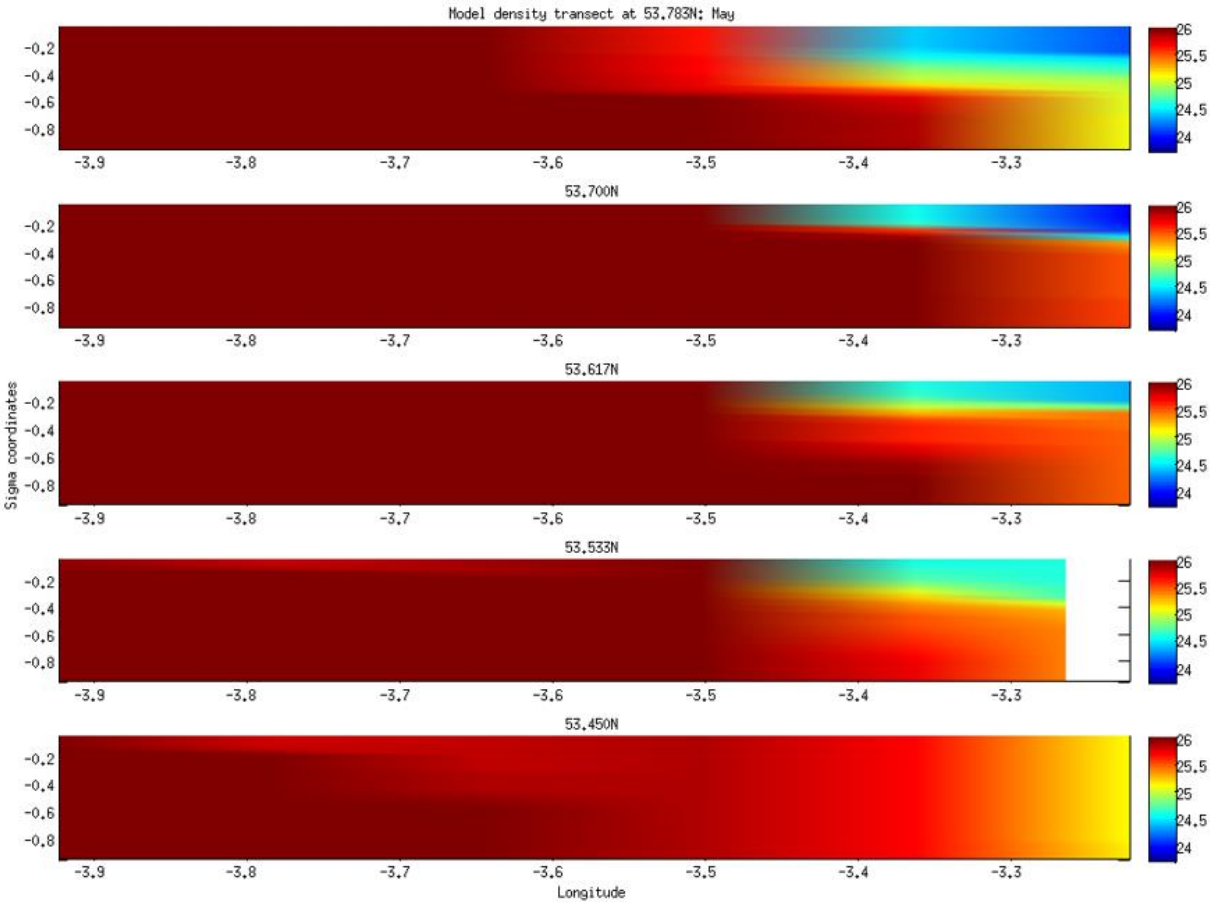

Figure 13: Transects 1-5 displaying model density on sigma levels in May.

Table 8: Error metrics for density transects 1-5 of the LB control run in May.

	HORIZONTAL			VERTICAL		
CTD: May DENSITY	Model Skill	Pbias	CF	Model Skill	Pbias	CF
1	0.58	-1.69	1.22	0.53	-66.09	0.83
2	0.53	-10.68	0.90	0.10	3.73	0.86
3	0.71	-39.17	0.47	0.41	18.74	0.57
4	0.89	-18.11	0.45	0.73	22.67	0.44
5	0.90	23.50	0.52	0.78	49.62	0.57

Figure 13 shows that the model correctly predicts a clear plume in transects 1-4 as observed, but it is constrained to the east and very shallow. The transects are therefore too saline causing an overall reduction in horizontal model skill in May (Table 8). Also, in contrast to January, transect 5 is now least well replicated with no stratification occurring in the model whereas in reality the plume spans the entire transect, which shows that the model is not capturing the structural variability of the front. This error may be explained by the Dee and Mersey plumes being disconnected in the model simulation (Fig. 17). Again the model shows a good low cost function across all transects in both directions, and in contrast with January, the horizontal density gradients are predominantly under-predicted in May.

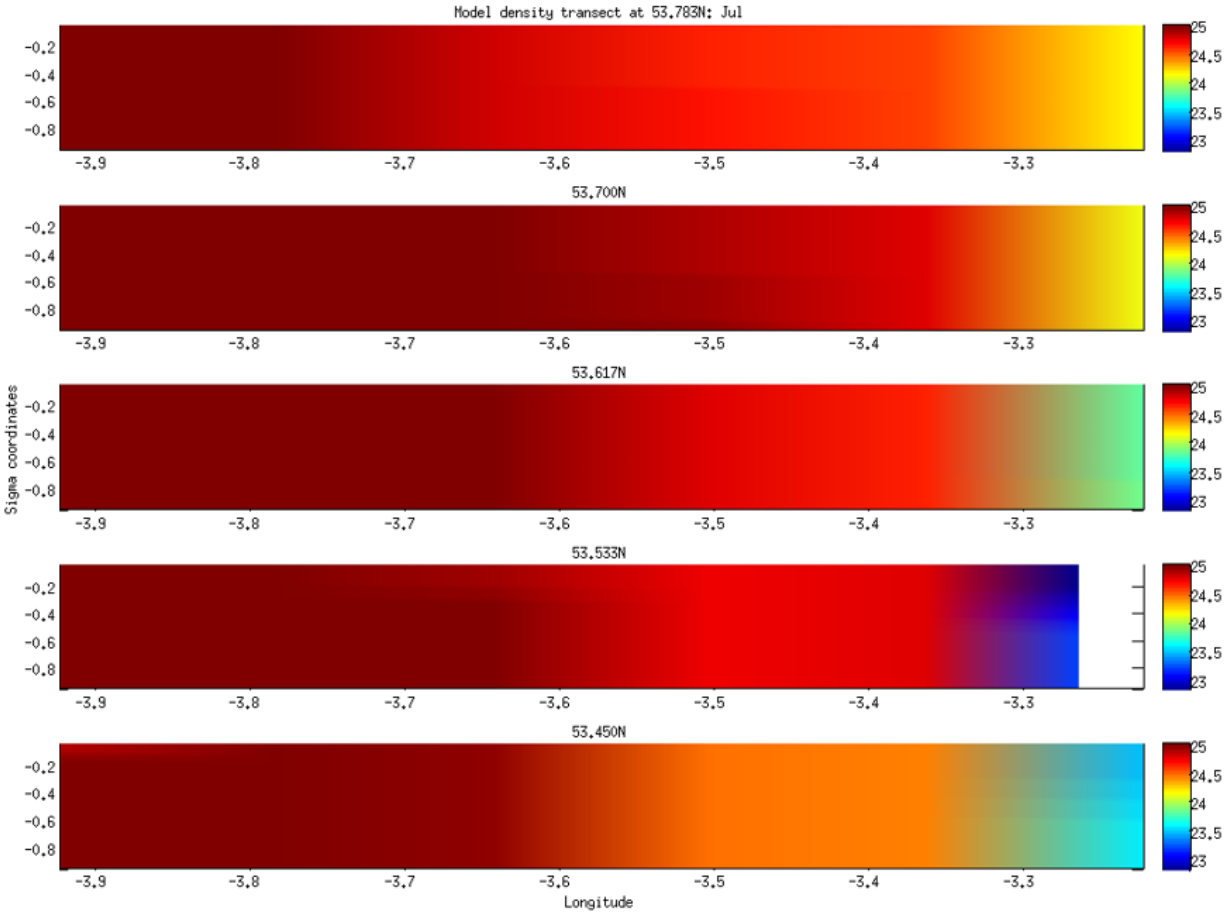

Figure 14: Transects 1-5 displaying model density on sigma levels in July.

Table 9: Error metrics for density transects 1-5 of the LB control run in July.

	HORIZONTAL			VERTICAL		
CTD: July DENSITY	Model Skill	Pbias	CF	Model Skill	Pbias	CF
1	0.72	-34.58	0.59	0.42	57.39	0.59
2	0.91	-28.40	0.36	0.37	84.53	0.69
3	0.92	-28.55	0.36	0.31	91.13	0.56
4	0.98	-2.40	0.27	0.78	49.13	0.55
5	0.96	-17.59	0.30	0.45	41.51	0.56

Figure 14 shows the model is vertically well mixed in July, resulting in the absence of a plume, in contrast with the observations, which clearly displays the front across the transects between -3.7 and -3.3°E. As shown by the Site A and B salinity validation (Figs. 4a and 5a), and the observational salinity transects (not shown), the near-surface offshore area of the LB model is too saline and therefore the density structure here is affected, reducing stratification. This inhibits the model's ability to correctly simulate the mixing front. This is most likely due to the model recovering too quickly from a freshet (reduction in salinity due to high river flow) during March (Fig. 5a, days 66-87), when a persisting stratified plume structure should be evident.

Table 9 shows high model skill due to the model's ability to replicate the overall horizontal density gradient, but the gradients between each site are slightly under-predicted. The vertical gradients towards the coast and offshore seem accurate, but the low resolution (6 CTD casts) of the data prevents the few points influenced by stratification significantly impacting the validation.

4.4 Local sensitivity to model parameter settings

To improve the nested LB model, first the parameter settings are investigated.

As model temperature validates well at Sites A and B (Figs. 4b and 5b) and density in Liverpool Bay is mostly influenced by salinity, the model salinity needs to be corrected in order to improve the position of the mixing front. Figure 5a shows that a dip in salinity occurred between 6th and 27th March 2008, followed by a slow recovery through to September, which is not sufficiently captured in the LB model, but is more evident in the salinity biased IRS model. This non-replicated dip means that salinity is particularly over-predicted during the summer months in the LB model. It is during these summer months that Hopkins and Polton (2012) suggest the plume should detach from the bottom over an annual cycle. This suggests that tidal mixing from the bottom is extending too high in the water column, since it has been shown that river temperature has little impact on results.

Despite being a less physically accurate model due to its lower resolution (1.8km) the IRS model performs better in replicating the mixing front position due to its representation of the freshwater intrusion leading to an improved horizontal gradient in nearshore salinity (Figs. 4a and 5a). This could be partially due to the estuaries being unresolved so the freshwater is input at the estuary mouth at 20psu, whereas the freshwater is input into the LB model at 0psu up-estuary, nearer to source. The lower resolution increases numerical diffusion in the horizontal causing more dispersion of the freshwater, resulting in a more diffuse front which closer resembles the observed front, but there is no structure, as in LB, due to bathymetric influence. The higher resolution LB model may therefore require more accurate and/or frequent river inputs in order to better reproduce observed salinity.

The existence and restriction of the freshwater plumes in the LB model suggests that the water is being over-mixed in the vertical reducing dispersion of the surface plume. A comparison of maps (Figs. 15 and 16) depicting the frequency of a mixed or unstable water column occurrence in both models in Liverpool Bay during 2008 confirms the LB model is more mixed in the vertical.

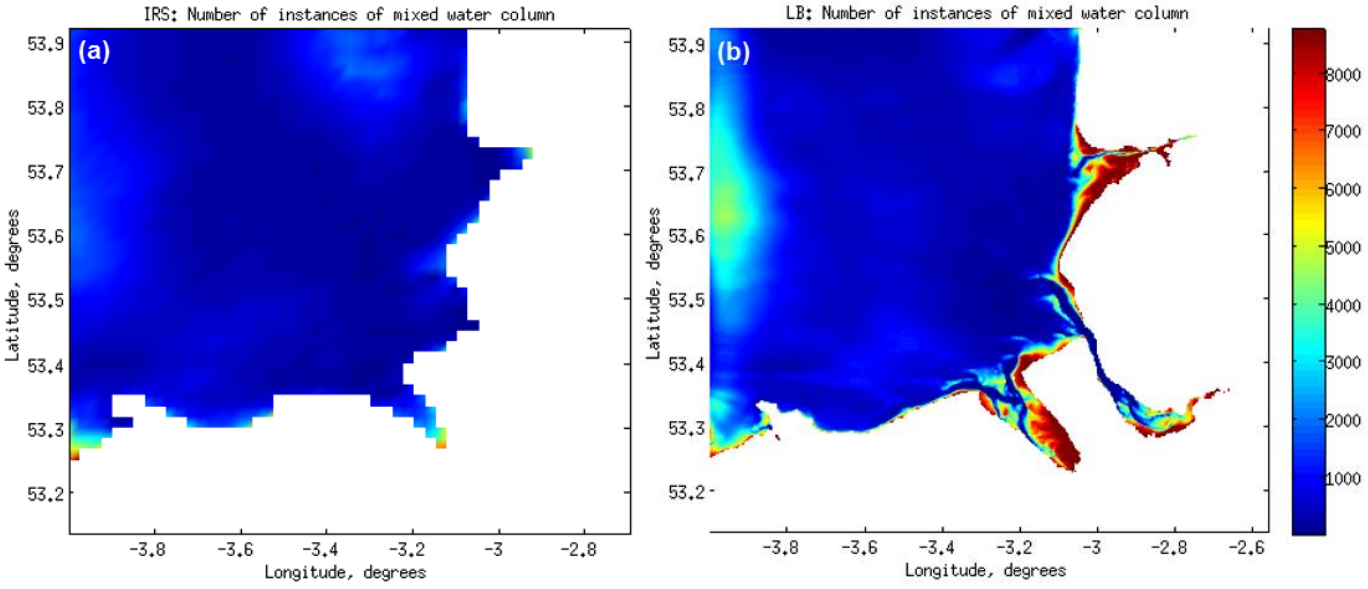

Figure 15: Annual (2008) occurrences of a mixed water (represented as a difference between surface and bottom salinity of 0) column across Liverpool Bay in POLCOMS applied to (a) the Irish Sea and (b) Liverpool Bay.

The LB model is more often vertically well mixed in the nearshore around Site B and the mouth of the river Dee (Fig. 15). This could explain why the Dee does not seem to contribute to the location of the nearshore front in this model, but does in the IRS model. The mixing is clearly related to the bathymetry as it increases with reduced depth.

Both models are often unstable with denser water over less dense (Fig. 16) and the maps of the frequency of mixed/unstable conditions seem to resemble the coastal bathymetry.

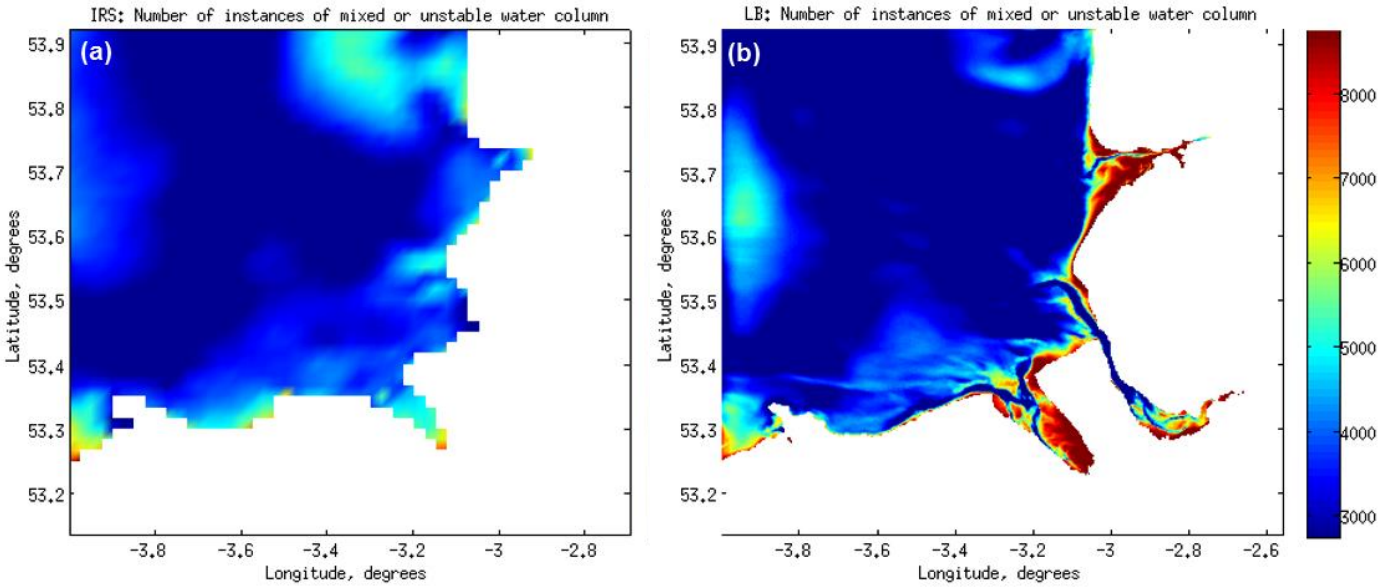

Figure 16: Annual (2008) occurrences (represented as a difference between surface and bottom salinity of ≤0) of a mixed or unstable (denser water on top of less dense) water column across Liverpool Bay in POLCOMS applied to (a) the Irish Sea and (b) Liverpool Bay.

In attempt to improve the location of the front, the local ROFI model setup is investigated by a sensitivity analysis of parameter settings. Table 10 lists the various amendments made to the model setup in an attempt to better replicate the observed front by enabling the freshwater to advect further offshore. For each of these simulations, a salinity surface map such as Figure 17b was created, and also time series at Sites A and B were plotted for temperature, salinity and density, as per Figure 2, to be compared with the control run. Each setup showed none or very little change to the model's capability so were rejected.

Table 10: Alterations to model setup trialled with little or no effect on model performance. Outputs are stored at: /projectsa/iCoast/Mersey_CEFAS/LB2008/sens_analysis.

Run name	Alterations to model setup	Switches used
CTD_horiz	Horizontal diffusion on z-levels included, with Smagorinsky (1963) coefficient set to 0.2 as suggested by Holt and James as optimal (2006).	HORIZDIF; HORIZTS
CTD_horiz1	As above, but with Smagorinsky coefficient increased to its maximum, 1.	As above
CTD_horizconst	Horizontal diffusion set to constant.	As above, with CONST_HORIZ_DIF
CTD_turbadv	Turbulence advection included.	TURBADV and an addition to the POLCOMS code
5mindepth	Minimum water depth increased from -10 to (+)5m to replicate the IRS setup.	hsmin altered in parameters.dat
Dee_bathy	Channel to Dee input location dug to ensure always wet; channels near estuary mouth deepened to further allow outflow.	
rivChannels	Mersey input location moved further down estuary (Fig. 15); Channels to Dee and Mersey input locations dug to ensure always wet.	Rivers_Mers_alt.index used in place of Rivers_JMB_ALE.index

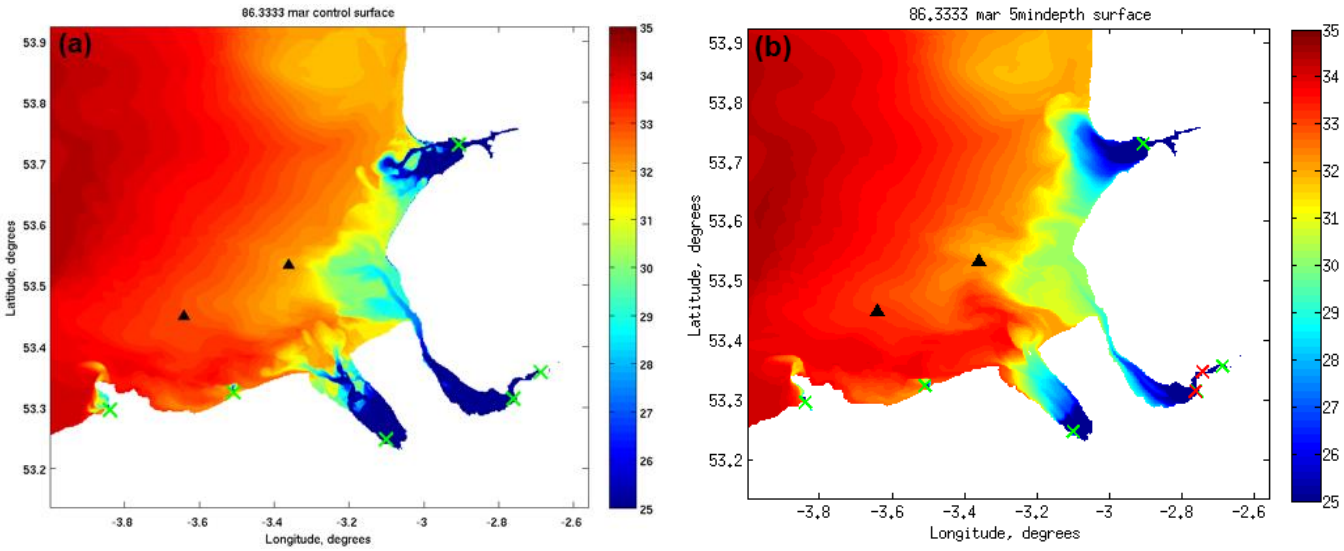

Figure 17: Model surface salinity at low water taken from POLCOMS applied to Liverpool Bay with (a) control setup and (b) minimum depth altered from -10m to 5m. Sites A and B are denoted by black triangles, the green crosses mark the original river input locations and the red crosses mark the new Mersey input locations.

Figure 17 highlights the importance of the estuary channels in constraining river flow at lower water elevation, causing the release of less saline water into the bay at low water.

For the model runs detailed in Table 11, the rivChannels bathymetry[5] and altered Mersey input location[6] (Fig. 17) remain as although they made little difference in getting the freshwater offshore, they do enhance the capability of the model by ensuring it is always possible for the freshwater to reach the estuary mouth. This is thought to be more realistic.

Table 11: Further alterations to model setup trialled with little or no effect on model performance

smooth5to18	rivChannels bathymetry smoothed between 5m (IRS minimum depth) and 18m depth. This region represents the complex coastal bathymetry.	
GOTMalt	Coefficient for length scale limitation in GOTM increased and decreased to represent different eddy length scales.	galp altered to 0.1, 0.5 and 1 from 0.267 in gotmturb.inp
GOTMscndmet2	Second order model type changed from "EASM with quasi-equilibrium" to "EASM with weak equilibrium, buoy.-variance algebraic".	scnd_method changed from 1 to 2 in gotmturb.inp
NOGOTM	GOTM switched off to test Mellor-Yamada (1982) mixing scheme, which is suspected to be less vigorous.	GOTM excluded from make command in make executable file

[5] /projectsa/iCoast/Mersey_CEFAS/LB2008/Danielle/LB_rivChannels_bathy_DN.txt
[6] /projectsa/iCoast/Mersey_CEFAS/Input_RIV/Rivers_Mers_alt.index

4.5 External sensitivity to boundary and initial conditions

Since the model was insensitive to the parameter settings, the boundary and initial conditions are investigated.

As manipulating the bathymetry, changing the mixing regime and switching both horizontal diffusion and turbulence advection on in POLCOMS still did not allow the required freshwater to advect far enough away from the coast to replicate the observed front, we examined the initial and boundary conditions. Previously, the LB initial salinity conditions had been biased by 1.15psu, in accordance with the IRS model optimum setup (Norman et al., 2014a), and the boundary conditions had been created from the optimum IRS run with the biased initial salinity of 1.15psu. To investigate the effect tuning the coarser IRS model had on performance of the nested higher resolution LB model, a LB simulation was setup with non-biased initial and boundary conditions. Model performance improves over much of the year, but the first three months before the dip in salinity are now significantly under-predicted (Figs. 18a and 19a).

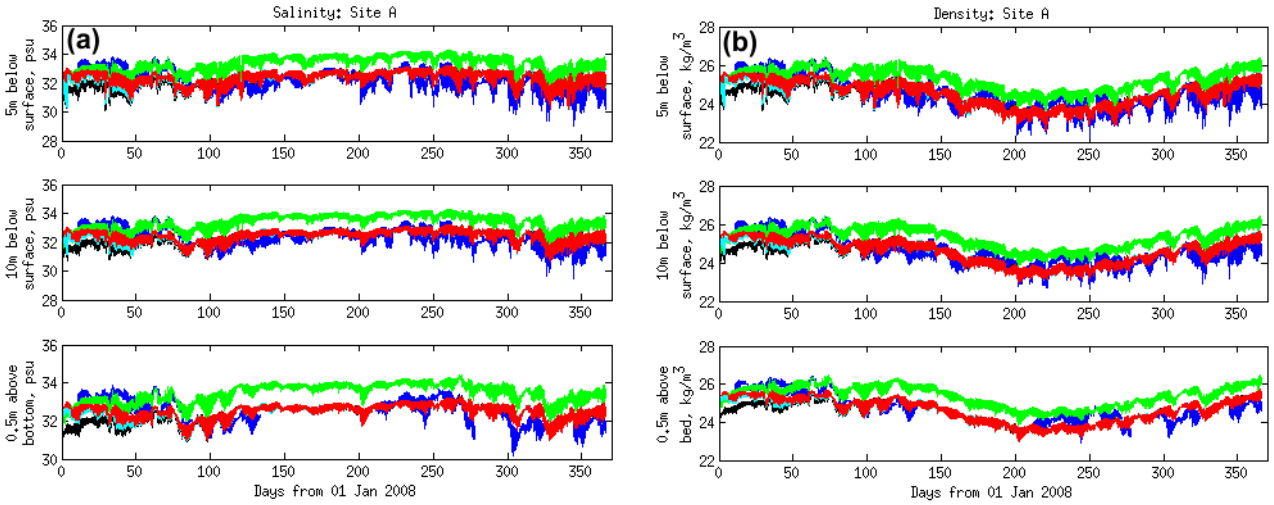

Figure 18: Annual (a) salinity and (b) density times series for observations (blue), LB control (green), unbiased initial and boundary conditions (black), initial bias of 1.15psu (cyan) and initial bias of 1.89psu (red), at Site A.

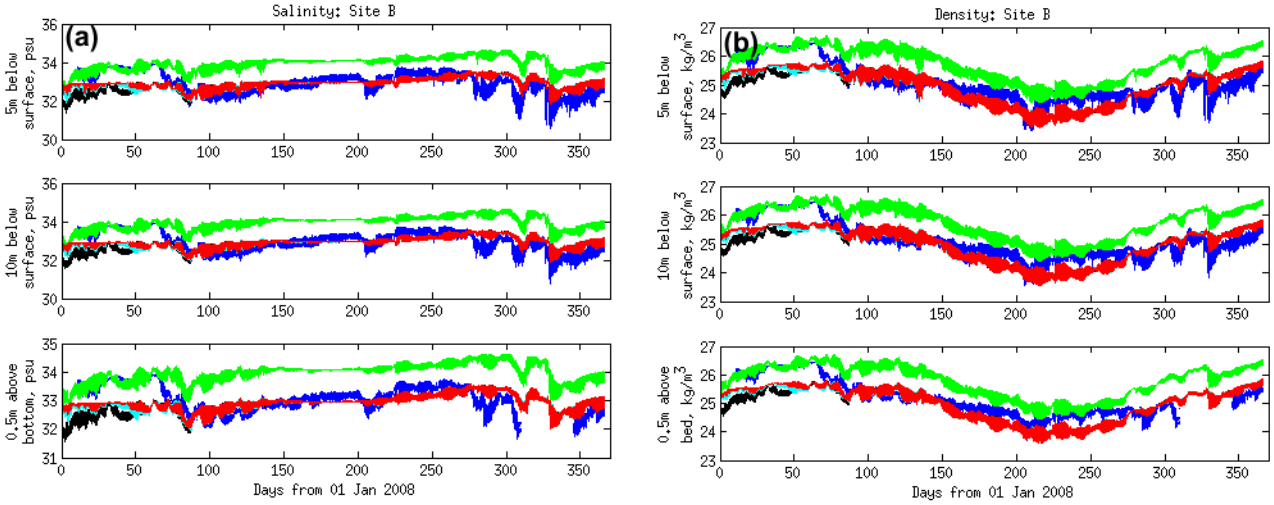

Figure 19: Annual (a) salinity and (b) density times series for observations (blue), LB control (green), unbiased initial and boundary conditions (black), initial bias of 1.15psu (cyan) and initial bias of 1.89psu (red), at Site B.

The re-inclusion of a 1.15psu bias in the initial salinity conditions, but with boundary conditions remaining unbiased, did improve model performance in the first three months at sites A and B, but not enough. This bias was increased to 1.89psu, calculated to be the mean difference between observed and model salinity across Sites A and B at the first instance of observational data recorded in January 2008. It

should be noted that the initial conditions only influence the first few months in the LB model, whereas they bias the full year in the IRS model (Figs. 2a and 3a). The LB domain is heavily influenced by the rivers and the coastal gradients rapidly adjust to the freshwater inflows.

It is evident that the boundary conditions are having a strong influence on the nearshore salinity as tuning the initial bias only influences the salinity at Sites A and B through January and February (Figs. 18a and 19a), whereafter the simulations converge back to the 'nobias' result. This suggests that the biased boundary conditions are more accurate until the large drop in salinity in March and the unbiased boundary conditions are more accurate for the rest of the year. In order to achieve an optimum simulation therefore, the boundary conditions would need to change around early March, but this is not advised as it would cause a discontinuous jump in salinity.

Figures 20-22 show the improvement in model performance when using non-biased initial and boundary conditions. All transects are now less dense, better replicating the observed density profiles. The density gradients are better replicated in January, as shown by the improvement in all error metrics in the horizontal and in many in the vertical (Table 12) despite the salinity, and therefore overall density, being under-predicted (Fig. 20).

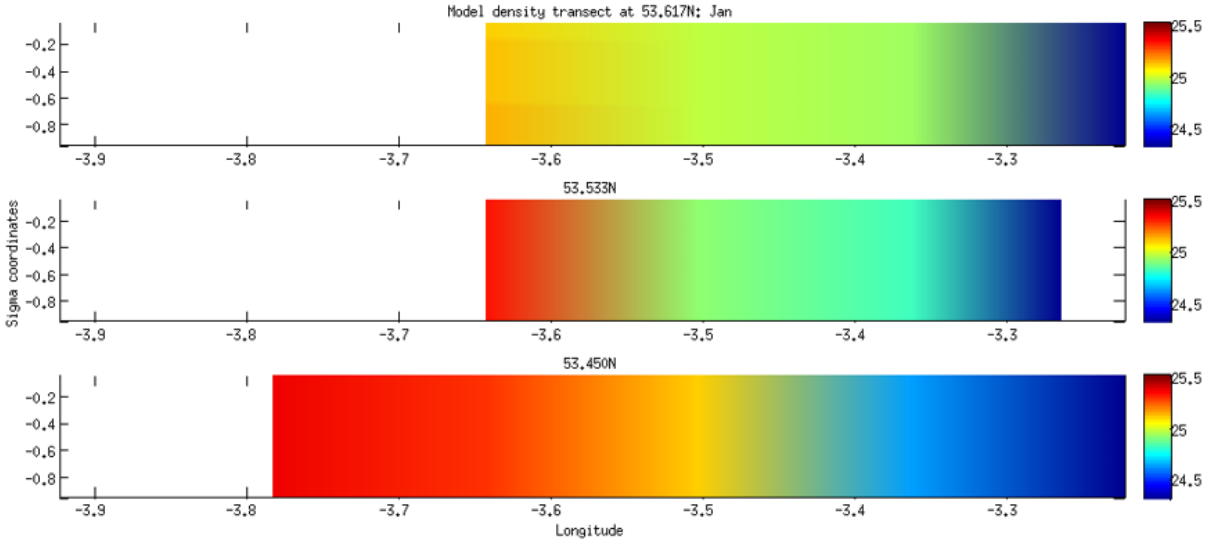

Figure 20: Transects 3-5 displaying model density on sigma levels in January. Taken from the nobias simulation. Note the colour scale has been reduced by 1kg/m^3 so cannot be directly compared with Figs. 9 & 12.

Table 12: Error metrics for density transects 3-5 of the LB nobias run in January. A value in red indicates performance equal to, and bold indicates performance better than, the control (biased) simulation.

	HORIZONTAL			VERTICAL		
CTD: Jan DENSITY	Model Skill	Pbias	CF	Model Skill	Pbias	CF
1	N/A	N/A	N/A	N/A	N/A	N/A
2	N/A	N/A	N/A	N/A	N/A	N/A
3	**0.93**	**31.24**	**0.48**	**0.13**	**-257.35**	**2.28**
4	**0.90**	**44.05**	**0.66**	0.60	49.38	**0.30**
5	**0.94**	**35.30**	**0.45**	**0.23**	96.62	**0.35**

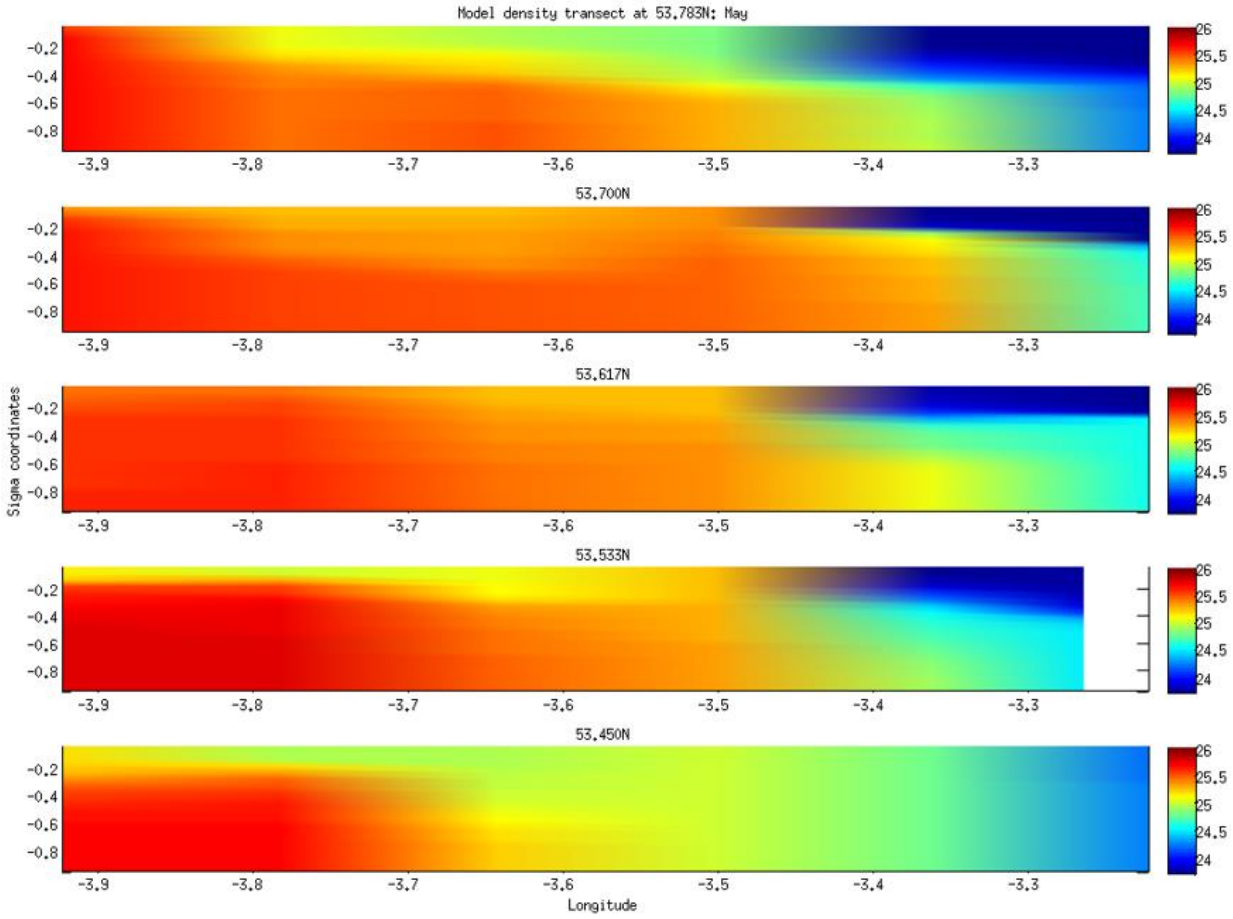

Figure 21: Transects 1-5 displaying model density on sigma levels in May. Taken from the nobias simulation.

In May, the model density profiles from the nobias simulation visibly better replicate those of the observed density, but the pycnocline is not as sharp as in reality. There are improvements in the N^2 error metrics, in both x- and y-directions.

Table 13: Error metrics for density transects 1-5 of the LB nobias run in May. A value in red indicates performance equal to, and bold indicates performance better than, the control (biased) simulation.

	HORIZONTAL			VERTICAL		
CTD: May DENSITY	Model Skill	Pbias	CF	Model Skill	Pbias	CF
1	0.56	-5.91	**1.13**	0.52	**-58.79**	0.86
2	0.49	-12.26	0.97	0.10	**2.79**	0.86
3	0.71	-40.68	**0.46**	**0.44**	19.37	**0.54**
4	**0.90**	-19.28	0.45	**0.79**	24.75	**0.40**
5	**0.92**	**20.92**	**0.48**	0.76	**49.33**	0.58

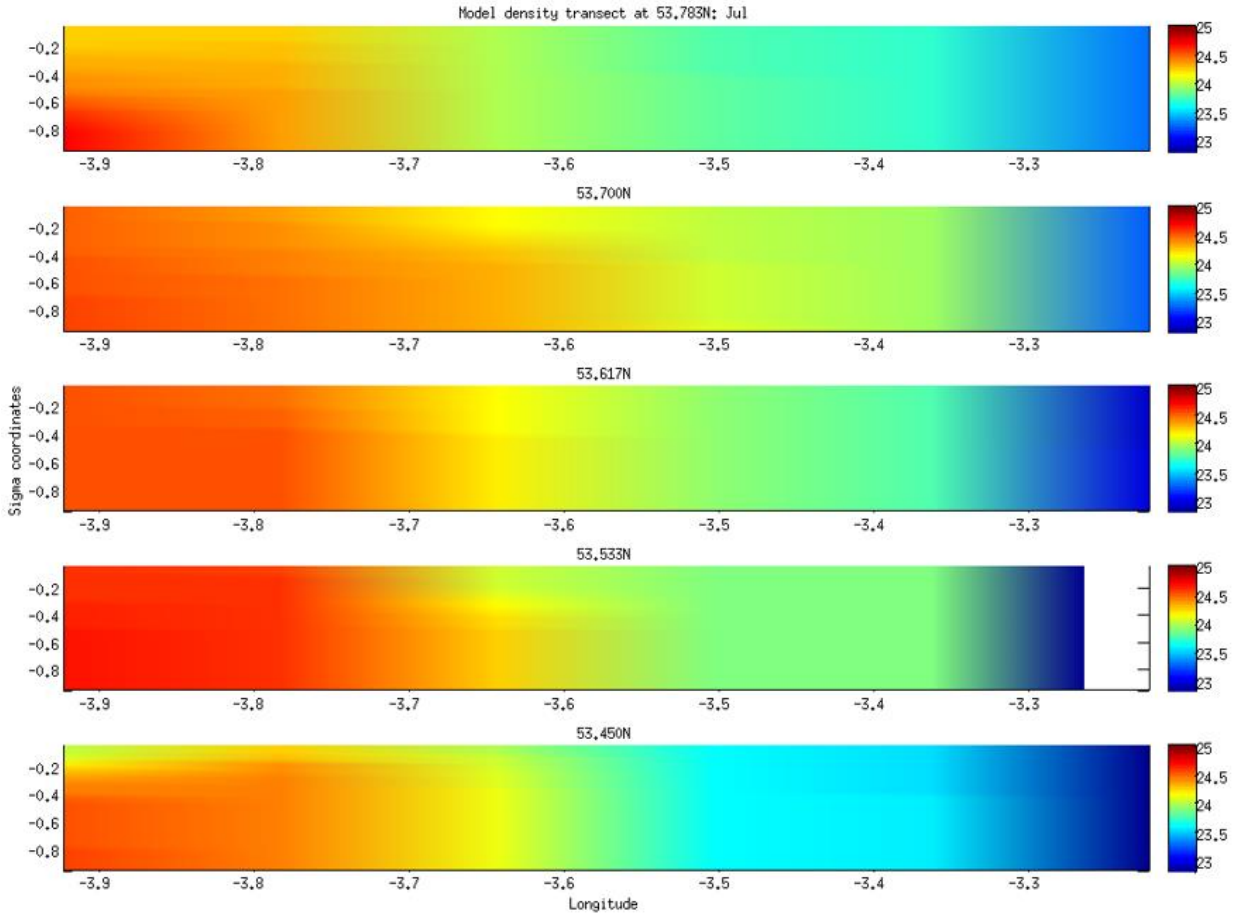

Figure 22: Transects 1-5 displaying model density on sigma levels in July. Taken from the nobias simulation.

The unbiased LB simulation also better replicates the observed horizontal density gradients in July (Fig. 22) and all of the transects show a reduction in Pbias in both directions, which supports this. However, the plume structure is now weaker and in some transects absent and the offshore density is also slightly too high.

Table 14: Error metrics for density transects 1-5 of the LB nobias run in July. A value in red indicates performance equal to, and bold indicates performance better than, the control (biased) simulation.

	HORIZONTAL			VERTICAL		
CTD: July DENSITY	Model Skill	Pbias	CF	Model Skill	Pbias	CF
1	0.71	**-33.88**	0.62	**0.45**	**55.05**	0.60
2	**0.92**	**-25.59**	**0.34**	0.37	**79.89**	**0.68**
3	0.92	**-27.86**	0.36	0.30	**86.00**	0.57
4	0.98	**-0.50**	**0.23**	0.78	**46.85**	0.55
5	**0.97**	**-15.55**	**0.28**	0.43	**29.66**	0.59

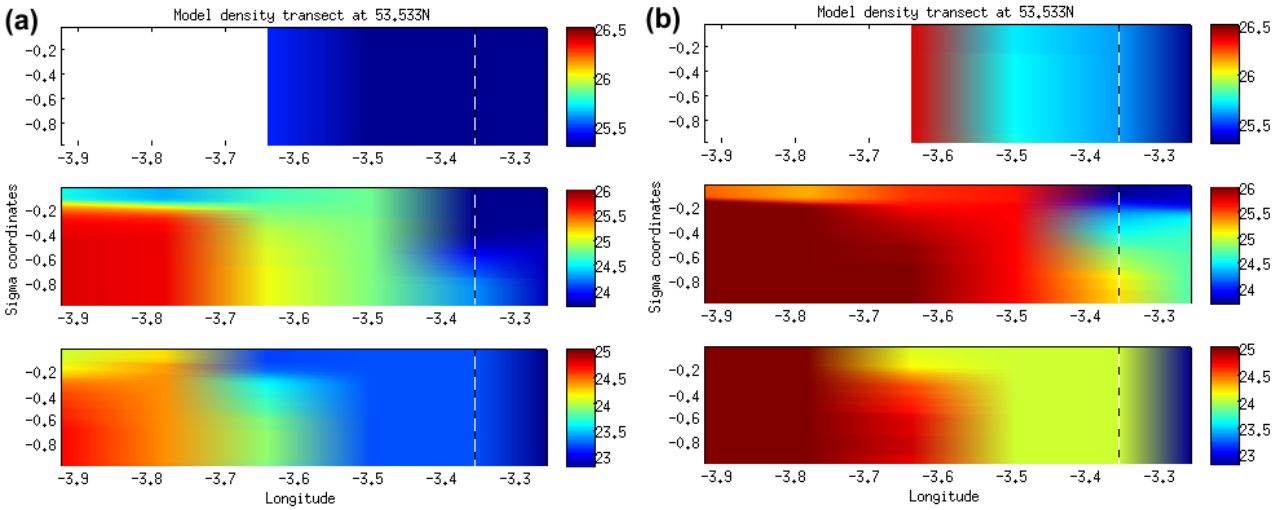

Figure 23: Density transect 4 taken from the Irish Sea model with (a) unbiased and (b) 1.15psu biased initial conditions in January (top), May (middle) and July (bottom). The location of Site A is marked by a dashed line.

Figure 23 shows the IRS model representation for unbiased (a) and biased (b) initial conditions. Only transect 4 is shown as this coincides with Site A and is most influenced by the river Mersey so it is a good transect to represent the offshore intrusion of freshwater influence. It is clear that the biased salinity prevents the freshwater from extending as far from the coast, which better replicates the observations. In May, the point at which the water becomes vertically well-mixed has moved towards the coast, but we also see an eastward intrusion of the offshore more saline water below the surface; while in July, it remains in a similar location. The IRS model replicates the observed vertical structure due to it having more vertical levels than the LB model, but the horizontal structure is poorly replicated as a result of the lower resolution. The bias in salinity has clearly increased density across the transects, but the gradients are similar over the observed cross-section as there is no significant difference between the error metrics for the two simulations (Tables 15 and 16). This suggests there could be a more significant change in gradients between the eastern limit of the CTD grid and the river source.

Overall, the IRS model is able to capture a plume structure. In comparison with the nested LB results (Figs. 12-14 and 20-22, panel 4), the density profiles are similar, but due to the lower resolution in the IRS model, there is less detail in the frontal structure near the coast allowing greater freshwater dispersion at the surface.

In addition to the biased IRS model performing better at Site A, the CTD grid transects close to Site A confirm that the density further offshore (-3.9°E) is also more accurate. The biased IRS model is therefore good at representing the ROFI. The LB biased results are over saline, which suggests that there could be errors in the offshore salinity in the IRS model at the LB boundary due to the bias. It is suggested that the unbiased IRS model did not have this offshore error and the higher resolution LB model was able to capture the dynamics of the ROFI, whereas the IRS model could not.

Table 15: Error metrics for the IRS control simulation.

IRS control: DENSITY		HORIZONTAL			VERTICAL		
		Model Skill	Pbias	CF	Model Skill	Pbias	CF
January	1	N/A	N/A	N/A	N/A	N/A	N/A
	2	N/A	N/A	N/A	N/A	N/A	N/A
	3	0.48	179.43	2.82	0.00	-4979.53	9.08
	4	0.96	16.56	0.29	0.31	83.61	0.10
	5	0.69	117.68	1.46	0.82	-9.80	0.06
May	1	0.79	0.11	0.73	0.42	54.64	0.10
	2	0.89	2.73	0.40	0.54	7.43	0.08
	3	0.86	6.12	0.42	0.38	-3.03	0.10
	4	0.76	3.55	0.77	0.28	6.13	0.10
	5	0.71	77.04	1.20	0.63	14.38	0.13
July	1	0.87	42.74	0.64	0.48	39.93	0.09
	2	0.92	32.18	0.44	0.37	72.00	0.10
	3	0.90	36.77	0.50	0.73	-40.76	0.12
	4	0.96	5.76	0.33	0.28	51.98	0.13
	5	0.93	31.11	0.50	0.70	-35.07	0.11

Table 16: Error metrics for the IRS simulation with an initial salinity bias of 1.15psu.

IRS bias: DENSITY		HORIZONTAL			VERTICAL		
		Model Skill	Pbias	CF	Model Skill	Pbias	CF
January	1	N/A	N/A	N/A	N/A	N/A	N/A
	2	N/A	N/A	N/A	N/A	N/A	N/A
	3	0.47	186.32	2.93	0.00	-5093.66	9.28
	4	0.95	18.26	0.30	0.31	82.93	0.10
	5	0.69	120.87	1.50	0.82	-15.69	0.06
May	1	0.70	5.51	0.82	0.43	49.55	0.10
	2	0.91	3.93	0.38	0.57	10.28	0.07
	3	0.86	8.56	0.43	0.38	-7.19	0.11
	4	0.75	6.43	0.80	0.29	3.79	0.10
	5	0.69	81.82	1.26	0.68	13.31	0.12
July	1	0.88	40.69	0.62	0.44	46.28	0.09
	2	0.92	33.41	0.43	0.36	75.16	0.10
	3	0.90	40.13	0.52	0.72	-39.63	0.13
	4	0.97	4.69	0.27	0.30	60.39	0.12
	5	0.92	31.15	0.52	0.72	-33.16	0.11

4.6 Surface salinity analysis

To understand why the models require different tuning, we investigate maps of the surface salinity at the lowest point of the salinity dip in March (Day 86.33, Fig. 4a) (Fig. 24). The maps were plotted at low water as this is the period at which stratification is greatest. During the ebb tide, the freshwater can move out from the estuary, advecting over the denser sea water away from the coast. Evidently, this freshwater is being inhibited in the LB model.

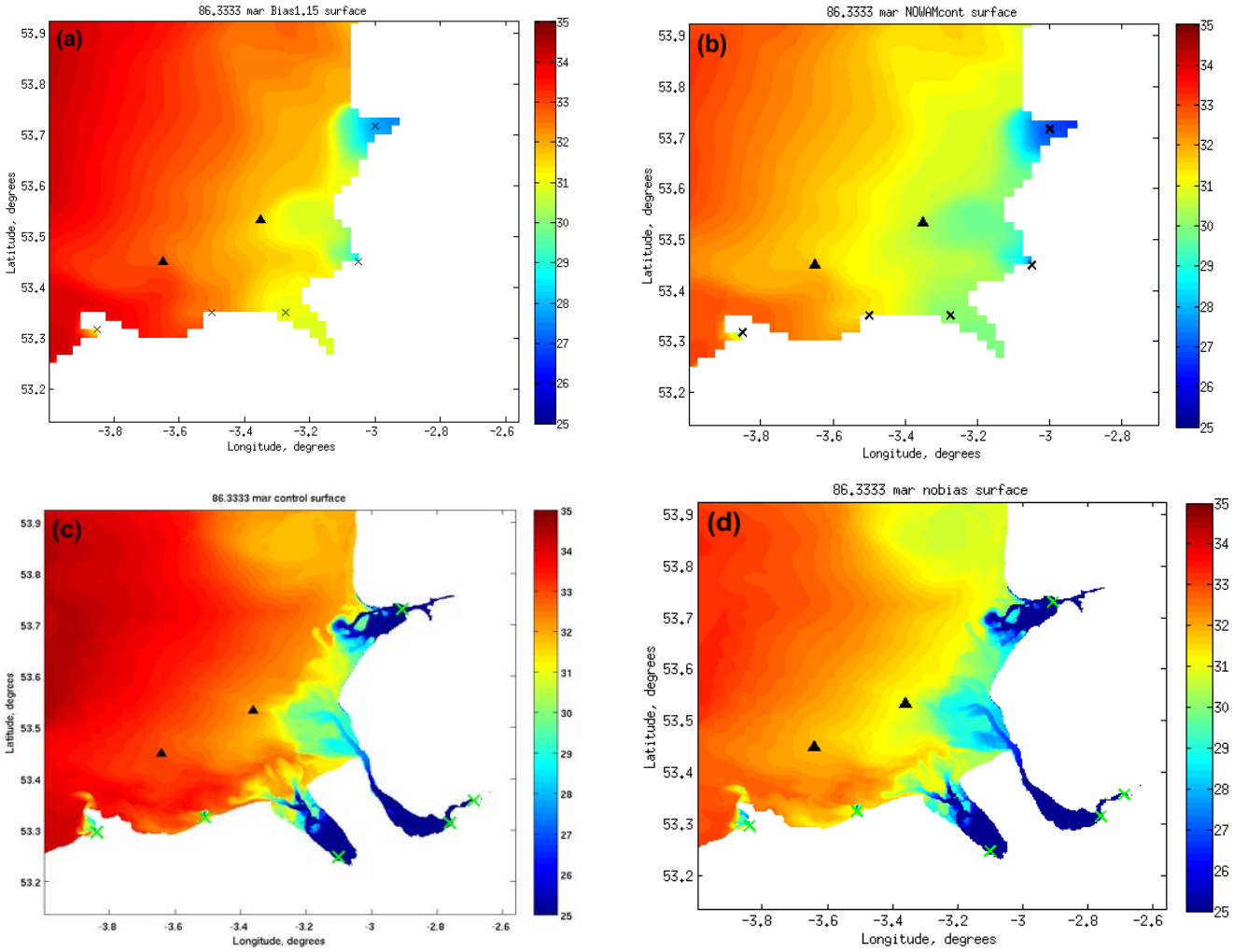

Figure 24: Model surface salinity in Liverpool Bay at low water taken from POLCOMS applied to: the Irish Sea with (a) 1.15psu salinity bias and (b) no bias; and to Liverpool Bay with (a) biased initial and boundary conditions and (d) no bias. Sites A and B are denoted by black triangles and the crosses mark the river input locations.

We can see from Figure 24b that a bias of 1.15psu in the initial salinity conditions was required in the IRS model to increase the offshore coastal ocean salinities increasing the density gradient and causing the ROFI to reduce. Consequently, the front forms closer to the coast improving the results for this model setup (Fig. 24a) at Sites A and B.

The LB model represents the ROFI; nesting into the biased IRS causes over saline boundary conditions preventing the freshwater intrusion into the bay (Fig. 24c). Using unbiased boundary conditions accurately represents the gradients capturing the plume intrusion (Fig. 24d). This shows the extent to which the ROFI is controlled by the offshore salinity.

4.7 Analyses of plume structure

Taking the best LB model set-up overall, with unbiased initial and boundary conditions, we examine the influence of the tide on plume structure in the bay.

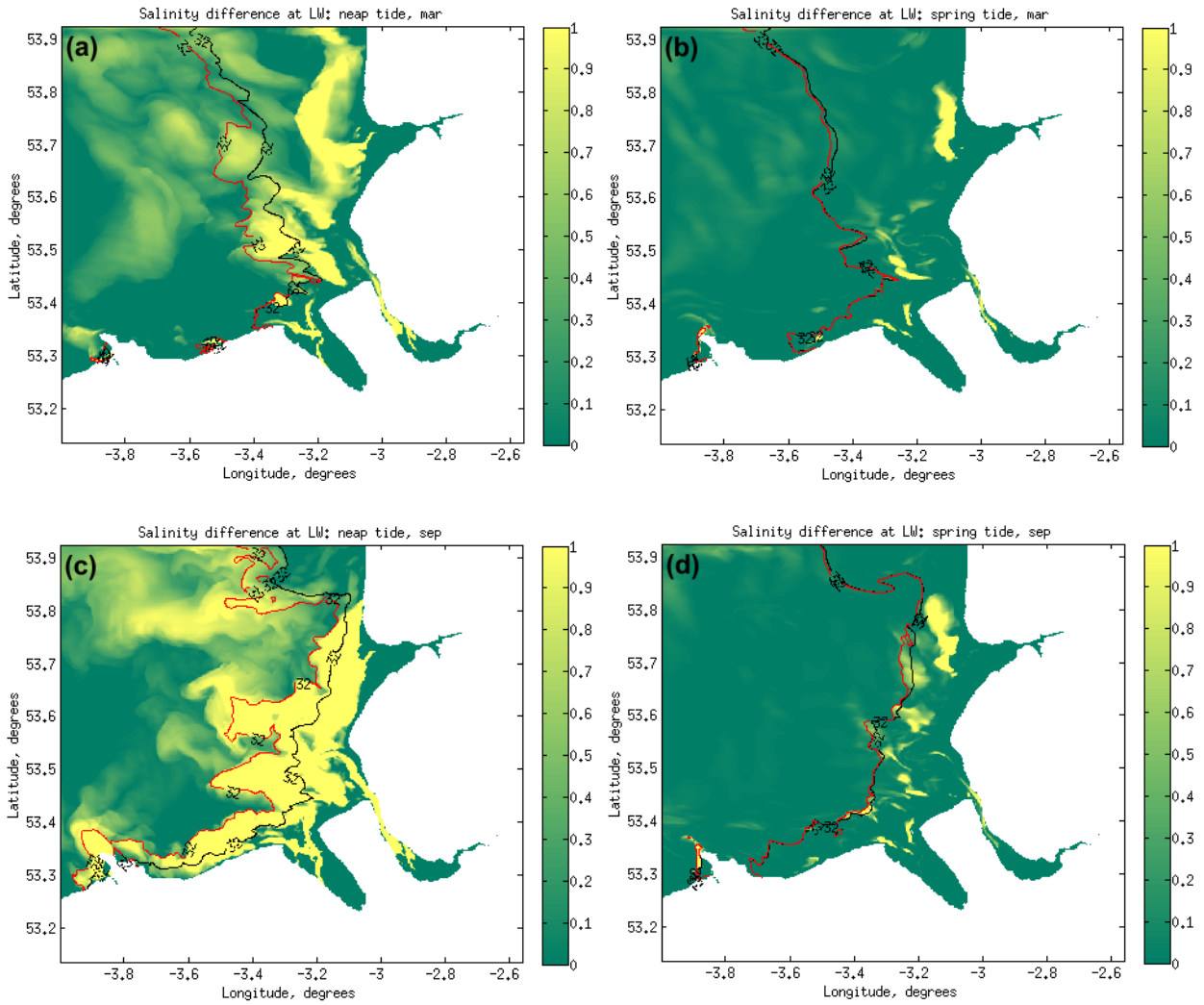

Figure 25: Difference between near-bed and surface salinity at low water (shown as the colour map) with surface (red) and bottom (black) 32psu contour in March during a (a) neap and (b) spring tide, and in September during a (c) neap and (d) spring tide. Taken from the nobias simulation.

Figure 25[7] shows that the spring tide, which is more energetic than the neap tide, results in the water being more vertically mixed as the surface 32psu contour lies on or very close to the near-bed contour. The plume, evident at neap tide in both months depicted, is more disperse in places for September than for March as shown by the greater distance between the surface and near-bed salinity contour. Low water has been chosen as following the ebb tide is when most stratification occurs.

[7] Scripts used: SAL_MAPS_DN.m; difference_map.m, located in /projectsa/iCoast/Mersey_CEFAS/LB2008/matlab

5. Future Work

Figure26 shows the location of two wind farms in Liverpool Bay. It also maps the surface salinity at the same time as investigated previously (Fig. 24) for a nobias model simulation with these wind farms included. At Sites A and B, the inclusion of the wind farms had negligible impact (Tables 17 and 18). However, we can see in Figure 26 that the river Dee plume is fresher than the previous nobias run (Fig. 24d) due to more mixing locally although it still does not connect to the river Mersey plume in this case. At this resolution, the wind farms are having a local influence, which shows the importance of considering man-made interventions at this scale.

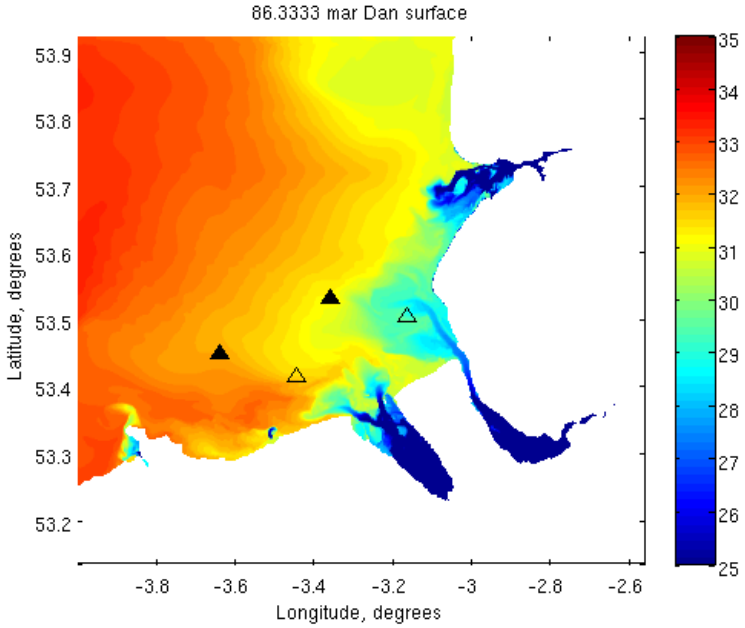

Figure 26: Surface salinity map taken from the LB nobias simulation with wind farms included. The black triangles represent Sites A and B and the clear triangles denote the location of the wind farms.

Table 17: Error metrics as per Table 1, for Site A and Site B: LB nobias run.

LB: nobias		Site A			Site B		
		Model skill	Bias	RMSE	Model Skill	Bias	RMSE
	u	0.97	0.00	0.14	0.98	0.01	0.11
	v	0.82	0.01	0.07	0.92	0.00	0.05
S	-5m	0.61	0.03	0.73	0.53	-0.09	0.58
	-10m	0.59	-0.02	0.68	0.54	-0.13	0.54
	Bottom	0.51	-0.14	0.76	0.48	-0.22	0.51
T	-5m	0.99	0.43	0.74	0.98	0.50	0.65
	-10m	0.99	0.47	0.74	0.98	0.49	0.65
	Bottom	0.99	1.23	1.06	0.98	0.35	0.72
ρ	-5m	0.85	-0.08	0.53	0.84	-0.18	0.44
	-10m	0.85	-0.12	0.50	0.84	-0.21	0.42
	Bottom	0.78	-0.36	0.57	0.85	-0.25	0.38

Table 18: Error metrics as per Table 1, for Site A and Site B: LB nobias run with wind farms included.

LB: nobias wind farms		Site A			Site B		
		Model skill	Bias	RMSE	Model Skill	Bias	RMSE
	u	0.97	0.00	0.14	0.98	0.01	0.11
	v	0.83	0.01	0.07	0.92	0.00	0.05
S	-5m	0.63	0.05	0.70	0.54	-0.09	0.58
	-10m	0.60	0.00	0.66	0.55	-0.12	0.54
	Bottom	0.52	-0.13	0.75	0.48	-0.21	0.52
T	-5m	0.99	0.44	0.74	0.99	0.51	0.62
	-10m	0.99	0.49	0.74	0.98	0.50	0.63
	Bottom	0.99	1.24	1.06	0.98	0.37	0.69
ρ	-5m	0.86	-0.06	0.51	0.84	-0.18	0.44
	-10m	0.86	-0.11	0.48	0.84	-0.20	0.41
	Bottom	0.79	-0.35	0.56	0.85	-0.25	0.38

6. Discussion and Conclusions

- Low sensitivity to river temperature suggests surface heating rather than river temperature enhances the buoyancy of the surface layer during stratified periods, having a stabilising influence on the plume and enabling further extension offshore.

- The IRS is controlled by shelf sea dynamics and the low model resolution increases horizontal diffusion as the front is strained under the tidal dynamics. To improve the representation of the ROFI in the IRS model, the initial salinity conditions need to be biased to compensate for numerical diffusion. However, this enhances the salinity across the full domain, which is not sensitive to coastal river flow. This then causes the external boundary conditions to a nested ROFI to be over saline, preventing the intrusion of the plume.

- Since the IRS model under-predicts the salinity of the ROFI under non-biased conditions, it is thought the initial conditions in the unbiased LB model require a salinity bias to counteract the over-diffused plume. Sensitivity analysis of different LB initial conditions shows, however, that the time series at sites A and B converge to that of the simulation with unbiased initial conditions.

- The initial conditions only have a short-term influence in the LB model since the domain is controlled by the freshwater plume, the extent of which is determined by the boundary conditions.

- In January, the LB boundary conditions taken from the biased IRS model are shown to be more accurate than the non-biased. This could be due to the more saline conditions compensating for the influence of the wind-driven evaporation, which is not considered in the model, as January is known to be a particularly windy month (Norman et al. 2014b).

- Validation of the time-varying conditions at sites A and B shows the importance of using the correct boundary conditions to enable accurate simulation of the time-varying freshwater inflow and how it disperses across the bay.

- Validation of the IRS model using the CTD grid shows the importance of considering observations at the offshore extent of the ROFI to ensure an appropriate coarse model setup is used to provide boundary conditions, as the best setup capturing conditions internally within the ROFI may be inaccurate further offshore. These results therefore show the need to validate the coarse model setup across its full domain to have confidence in the offshore and nearshore conditions. It is very unusual, however, to have access to observations that cover such spatial scales.

- The LB model clearly resolves more structure of the front, capturing the wavy features of the plume and bathymetric influence.

- It is difficult to validate the front due to the need to capture spatial variability in gradients and a property's magnitude. Here, error metrics are used to focus on the vertical and horizontal gradients, as there could be errors in the magnitudes due to limitations in the river forcing. Resolution of the spatial structure may be limited by the number of observations, especially in the horizontal. In addition, the timing of the observations does not allow an instantaneous snapshot of a tidal phase. The limitations of the observations again make validation difficult.

- In January, stormy weather occurred around spring tides and we see that the water column is well mixed with a horizontal density gradient across the transects. In May and July, in calmer, warmer conditions, a freshwater plume is evident causing more stratification during mean to

neap tides. It is thought that the plume formation (seen in the CTD density profiles) may therefore be related to the coincident tidal regime rather than the seasonal cycle.

- Less saline boundary conditions in the LB model cause the plume to extend further offshore, improving the CTD density profiles in May and July. More saline initial conditions reduce the model skill and increase bias in capturing the horizontal density gradients between CTD sites in January.

- The local dynamics in LB are insensitive to the local parameter settings and bathymetry. The ROFI dynamics are controlled by density gradients. Extra computation had a large influence on run time, which was not compensated for by improved simulation. When including turbulence advection, the time step ratio was also changed for stability, which added extra time:

Executable name	Run time: January 2008
CTD_control	4.5 hours
CTD_horizdif	8.75 hours
CTD_turbadv	9.82 hours

- Using accurately biased initial salinity conditions in the IRS model increases the salinity for the whole year, which is inaccurate offshore but compensates for numerical diffusion over-predicting the region that the freshwater influences.

- In the LB model, the higher resolution corrects the numerical diffusion thus accurate boundary conditions and initial temperature and salinity conditions are required. The initial conditions only influence the first few months in LB as the freshwater inflow controls the dynamics. The annual bias in IRS in response to initial salinity shows that the coastal sea experiences minimal influence from coastal freshwater.

- It is clear that horizontal grid resolution is very important for accurate simulation of a ROFI. A high resolution (~180 m) is required to prevent numerical diffusion over-predicting the dispersion of the freshwater. It is also important to be aware of the limitations of the coarser models in a nested system to obtain the correct initial and boundary conditions.

- In the LB model, the inclusion of wind farms is shown to have a local influence, which shows the importance of considering man-made interventions at this scale.

6. References

Allen, J.I., Holt, J.T., Blackford, J., Proctor, R., 2007. Error quantification of a high-resolution coupled hydrodynamic-ecosystem coastal-ocean model: Part 2. Chlorophyll-a, nutrients and SPM. Journal of Marine Systems 68, 381–404.

Canuto, V.M., Howard, A., Cheng, Y., Dubovikov, M.S., 2001. Ocean turbulence. Part I: One-point closure model – Momentum and heat vertical diffusivities. Journal of Physical Oceanography 31, 1413-1426.

Dyer, K.R., 1997. Estuaries: A Physical Introduction. John Wiley and Sons Ltd, Chichester, ISBN 0-471-9741-4 xiv, 195.

Holt, J.T., I. D. James, 2001. An S coordinate density evolving model for the northwest European continental shelf. Model description and density structure. Journal of Geophysical Research: Oceans, 106(C7), 14015–14034.

Holt, J.T., I. D. James, 2006. An assessment of the fine-scale eddies in a high-resolution model of shelf seas west of Great Britain. Ocean Modelling 13, 271-291.

Hopkins, J., Polton, J.A., 2012. Scales and structure of frontal adjustment and freshwater export in a region of freshwater influence. Ocean Dynamics 62, 45-62.

Howarth, M.J., Palmer, M.R., 2011. The Liverpool Bay coastal observatory. Ocean Dynamics 61, 1917-1926.

Mellor, G.L., Yamada, T., 1982. Development of a turbulence closure model for geophysical fluid problems. Reviews of Geophysics 20(4), 851–875.

Norman, D., Brown, J.M., Amoudry L.O., Souza A.J., 2014a. POLCOMS sensitivity analysis to river temperature proxies, surface salinity flux and river salinity in the Irish Sea. National Oceanography Centre Internal Document, No. 08, 22pp.

Norman, D., Brown, J.M., Amoudry L.O., Souza A.J., 2014b. Was 2008 a typical year in Liverpool Bay? National Oceanography Centre Internal Document, No. 09, 19pp.4 015–14 034.

O'Neill, C.K., Polton, J.A., Holt, J.T., O'Dea, E.J., 2012. Modelling temperature and salinity in Liverpool Bay and the Irish Sea: sensitivity to model type and surface forcing. Ocean Science 8, 903–913.

Polton, J.A., Palmer, M.R., Howarth, M.J., 2011. Physical and dynamical oceanography of Liverpool bay. Ocean Dynamics 61, 1421-1439.

Simpson, J.H., Brown, J., Matthews, J., Allen, G., 1990. Tidal straining, density currents, and stirring in the control of estuarine stratification. Estuaries 13, 125-132.

Smagorinsky, J., 1963. General circulation experiments with the primitive equations. Monthly Weather Review 91, 99-164.

Souza, A.J., 2013. On the use of the Stokes number to explain frictional tidal dynamics and water column structure in shelf seas. Ocean Science 9, 391–398.

Willmott, C.J., 1981. On the validation of models. Physical Geography, 2(2), 184-194.

Appendix 1

CTD Site	Lat (N)	Lon (W)	Transect	
2	53° 37′	3° 13.4′	3	
3	53° 42′	3° 13.4′	2	
4	53° 47′	3° 13.4′	1	
5	53° 52′	3° 21.8′	N/A	
6	53° 47′	3° 21.8′	1	
7	53° 42′	3° 21.8′	2	
8	53° 37′	3° 21.8′	3	
1/9	53° 32′	3° 21.8′	4	Site A
10	53° 27′	3° 13.4′	5	
11	53° 27′	3° 21.8′	5	
12	53° 27′	3° 30.2′	5	
13	53° 32′	3° 30.2′	4	
14	53° 37′	3° 30.2′	3	
15	53° 42′	3° 30.2′	2	
16	53° 47′	3° 30.2′	1	
17	53° 47′	3° 38.6′	1	
18	53° 42′	3° 38.6′	2	
19	53° 37′	3° 38.6′	3	
20	53° 32′	3° 38.6′	4	
21	53° 27′	3° 38.6′	5	Site B
22	53° 23′	3° 38.6′	N/A	
23	53° 23′	3° 47.0′	N/A	
24	53° 27′	3° 47.0′	5	
25	53° 32′	3° 47.0′	4	
26	53° 37′	3° 47.0′	3	
27	53° 42′	3° 47.0′	2	
28	53° 47′	3° 47.0′	1	
29	53° 47′	3° 55.4′	1	
30	53° 42′	3° 55.4′	2	
31	53° 37′	3° 55.4′	3	
32	53° 32′	3° 55.4′	4	
33	53° 27′	3° 55.4′	5	
34	53° 22′	3° 55.4′	N/A	
35	53° 32′	3° 15.9′	4	

NB: Site A was setup as station 1 prior to the CTD monitoring. When the grid surveys began, Site A was renamed station 9 and thus has a double number system. Site B was deployed after the implementation of the survey grid so only has one station number consistent with the CTD grid

Appendix 2

Cruise	Sites visited (in order)
10th-11th Jan 2008	10, 35, 2, 4, 8, 9, 11, 12, 21, 20, 19, 14, 13, 1(9), 1, 21, 21, 24
13th-16th May 2008	1 (25-hour survey) 10, 35, 2-21, 22-34
30th-31st July 2008	1 10, 35, 2-9, 11-21, 22-34